

Large Intelligent Surface/Antennas (LISA) Assisted Symbiotic Radio for IoT Communications

Qianqian Zhang, Ying-Chang Liang, *Fellow, IEEE*, and
H. Vincent Poor, *Fellow, IEEE*

Abstract

To support super-massive access for future wireless communications, in this paper, we propose a novel *large intelligent surface/antennas* (LISA)-assisted *symbiotic radio* (SR) system in which a LISA, operating as an Internet-of-Things (IoT) device, transmits messages to an *IoT receiver* (IR) by using reflecting radio technique, and at the same time, it assists the primary transmission from a *base station* (BS) to a *primary receiver* (PR) by intelligently reconfiguring the wireless environment. We are interested in the joint design for active transmit beamforming at BS and passive reflecting beamforming at LISA to minimize the total transmit power at BS, subject to the *signal-to-noise-ratio* (SNR) constraint for the IoT communication and the rate constraint for the primary transmission. Due to the non-convexity of the formulated problem, for the general case, we decouple the original optimization problem into a series of subproblems using the alternating optimization method and solve them one by one based on *KarushKuhnTucker* (KKT) conditions and projection method. For the special case in which the direct links from BS to PR and IR are blocked, we decouple the formulated optimization problem into two subproblems, one of which is a *semi-definite program* (SDP) problem and the other is solved by using *semi-definite relaxation* (SDR) technique. The convergence performance and the computational complexity of the proposed algorithms are analyzed for both cases. Finally, simulation results are presented to validate the effectiveness of the proposed algorithms and the superiority of the proposed system.

This work is supported in part by the National Natural Science Foundation of China under Grant 61631005, Grant U1801261, National Key Research and Development Program of China under Grant 2018YFB1801105, and 111 International Collaboration Project under Grant B20064, and in part by the U.S. National Science Foundation under Grant CCF-0939370 and Grant CCF-1513915. Part of the work will be presented in IEEE WCNC 2020 [1] (*Corresponding author: Ying-Chang Liang.*)

Q. Zhang is with the National Key Laboratory of Science and Technology on Communications, and the Center for Intelligent Networking and Communications (CINC), University of Electronic Science and Technology of China (UESTC), Chengdu 611731, China (e-mail: qqzhang_kite@163.com).

Y.-C. Liang is with the Center for Intelligent Networking and Communications (CINC), University of Electronic Science and Technology of China (UESTC), Chengdu 611731, China (e-mail: liangyc@ieee.org).

H. V. Poor is with the Department of Electrical Engineering, Princeton University, Princeton, NJ 08544 USA (e-mail: poor@princeton.edu).

Index Terms

Large intelligent surface/antennas (LISA), symbiotic radio (SR), beamforming, Internet-of-Things (IoT) communications, massive access.

I. INTRODUCTION

With the explosive growth of the *Internet-of-Things* (IoT) networks, the *beyond 5G* wireless systems need to support tens or even hundreds of access devices per square meter [2], [3], which is a very challenging task from both energy-efficiency and spectrum-efficiency perspectives [4]. Specifically, there will not be enough radio spectrum to support the dense and massive access if dedicated spectrum is allocated. In addition, the power consumption will be another critical problem if conventional active *radio-frequency* (RF) technology is used for transmitter design. *Ambient backscatter communication* (AmBC) is a promising solution to overcome these challenges. In particular, using AmBC technology, the IoT networks can parasitize in a primary network, and the IoT devices can transmit their messages to their destinations by riding over the RF signals received from an ambient (primary) transmitter with reflecting radio technology [5], [6]. That is to say, the IoT devices do not require dedicated RF emitters, and share the same spectrum with the primary system. Thus, AmBC is a potentially spectrum-efficient, energy-efficient, and low-cost technology for massive access, and it has attracted increasing attention from both academia and industry in the past decade [5]–[13].

There are two types of AmBC systems: non-cooperative AmBC and cooperative AmBC. For non-cooperative AmBC, there is no cooperation between the primary transmission and IoT communication, and thus each of them treats the other as interference [5]. In addition, due to the non-cooperation nature, the *IoT receiver* (IR) has limited knowledge about the primary transmission, and thus non-coherent detection such as energy detection is commonly used to recover the message of the IoT device, which will suffer from a huge performance loss since all the phase information of the received signals at IR is lost, e.g., [6]–[8]. To tackle the drawback of non-cooperative AmBC, cooperative receiver is used in [9] to coherently and jointly decode the messages from the primary transmitter and IoT devices. Interestingly, not only the performance of the IoT communication is improved, but also the performance of the primary transmission can be enhanced by using the cooperative receiver since the backscatter links from the IoT devices can be treated as additional multi-path due to the low-rate IoT transmission [9]. The system capacity study of cooperative AmBC in [10], [11] has further revealed that, with the cooperation between the primary transmission and the IoT communication, the capacity of the primary system can be enhanced and the IoT system obtains the transmission opportunity without requiring additional spectrum. Due to the mutualism relationship between them, *symbiotic radio* (SR) is proposed from a biological perspective [11], [14]–[17], which not only supports the IoT communication,

but also enhances the primary transmission. Specifically, the ergodic rate and the outage probability are analyzed for a symbiotic system of cellular and IoT networks in [14]. The resource allocation and transceiver design are studied in [11], [15], [16] to enhance the performance of SR system. The user association problem is studied in [17] to link each IoT device to a cellular user by using deep reinforcement learning.

However, because of the double fading effect, the backscatter link in SR is much weaker than the direct link, the performance improvement to the primary system may not be so significant. In this paper, we propose a *large intelligent surface/antennas* (LISA)-assisted SR system to enhance the backscatter link through reflecting beamforming, thus to enhance the performance of both primary and IoT transmissions. LISA, also known as *intelligent reflecting surface* (IRS) [18], [19], is a two-dimensional artificial structure including multiple reflecting elements with high controllability to achieve promising properties, such as negative reflection, perfect lensing, and perfect absorption [20]. Due to the unusual properties of LISA, the wireless environment can be soft-defined based on a specific requirement, and thus the coverage area can be extended and the power consumption can be reduced with the use of LISA, especially for the high-frequency band. Thus, LISA has been actively studied recently to assist wireless transmissions [21]–[29]. Specifically, in [21], the authors study the joint active and passive beamforming design problem to maximize the achievable rate for the single-user case, where the active beamforming refers to the transmitter design and the passive beamforming refers to LISA design. The downlink multiuser case is studied in [22] to minimize the total transmit power. In [23], transmit power allocation and passive beamforming are jointly designed to maximize energy efficiency. LISA-assisted physical layer security problem is studied in [24] to achieve high-efficiency secret communication. LISA-assisted *non-orthogonal multiple access* (NOMA) system is studied in [25], [26] and LISA-assisted MIMO system is studied in [27], [28]. In [29], the authors study the *simultaneous wireless information and power transfer* (SWIPT) using LISA.

Different from the above studies on LISA, which is used to purely assist the transmissions of other systems, the LISA-assisted SR system proposed in this paper is not only used to assist the primary transmission, but also to enhance the IoT communication. Specifically, in such a system, LISA as an IoT device transmits message to the IR by riding on the signals emitted from a *base station* (BS), and simultaneously, it assists the transmission of the primary system by intelligently reconfiguring its reflecting coefficients. We are interested in the SR system consisting of a multiple-antenna BS, a multiple-antenna *primary receiver* (PR), a LISA-assisted IoT device with multiple reflecting elements, and a multiple-antenna IR. Since both PR and IR receive two types of signals: direct link signal from BS and backscatter link signal from LISA, our objective is to jointly design the active transmit beamforming at BS and the passive reflecting beamforming at LISA such that the total transmit power at the BS is minimized, subject to the rate constraint for the primary

transmission and the *signal-to-noise-ratio* (SNR) constraint for the IoT communication. Due to the non-convexity of the formulated problem, for the general case, we decouple the optimization problem into a series of subproblems using the *alternating optimization* (AO) method and solve them one by one. Note that the number of subproblems equals the number of reflecting elements plus one. For the special case in which the direct links from BS to both PR and IR are blocked, we decouple the optimization problem into two subproblems using the AO method. These two subproblems optimize the active transmit beamforming matrix and the passive reflecting beamforming matrix, respectively, with the other variable fixed, one of which is solved by using *semi-definite relaxation* (SDR) technique. Since the reflecting coefficients are designed jointly, the convergence rate will be accelerated and the stability will be improved for the algorithm of the special case. The main contributions of this paper are summarized as follows.

- We propose a novel LISA-assisted SR system, which assists the primary transmission and IoT communication simultaneously.
- We analyze the principles of LISA to understand how LISA works and what effect LISA achieves for the SR system.
- The joint active transmit beamforming and passive reflecting beamforming design problem is formulated to minimize the total transmit power under a given rate constraint for the primary transmission and a given SNR constraint for the IoT communication.
- The AO method is used to solve the formulated optimization problem, in which the original problem is decoupled into a series of subproblems for the general case and into two subproblems for the special case.
- Finally, the simulation results are presented to validate the performance of the studied system and proposed algorithms. It is shown that by introducing LISA to the SR system, the performance of both primary and IoT transmissions can be enhanced significantly.

The rest of the paper is organized as follows. In Section II, we establish the LISA-assisted SR system model. In Section III, we explore the beamforming principles of LISA and illustrate the rationality of LISA for the SR system. In Sections IV, we formulate the power minimization problem for the general case. A special case that the direct links from BS to PR and IR are blocked is considered in Section V. Section VI presents simulation results for performance comparison to validate the effectiveness of the proposed algorithms and the superiority of the proposed system. Finally, the paper is concluded in Section VII.

The notations used in this paper are listed as follows. The lowercase, boldface lowercase, and boldface uppercase letters x , \mathbf{x} , and \mathbf{X} denote a scalar variable (or constant), vector, and matrix, respectively. $\mathcal{CN}(\boldsymbol{\mu}, \boldsymbol{\Sigma})$ denotes the complex Gaussian distribution with mean $\boldsymbol{\mu}$ and variance $\boldsymbol{\Sigma}$. \mathbf{X}^T , \mathbf{X}^\dagger , and \mathbf{X}^H denote the

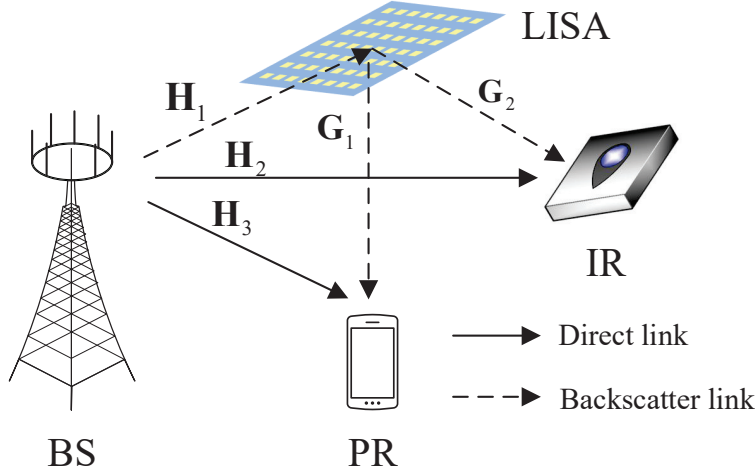


Fig. 1: The system model for LISA-assisted SR: LISA as an IoT device transmits message to IR by using the reflecting radio technology and assists the primary transmission from BS to PR.

transpose, conjugate, and conjugate transpose of matrix \mathbf{X} , respectively. Notation \mathbf{X}^* denotes the optimal value of variable \mathbf{X} . \mathbf{I}_N denotes the N -dimensional identity matrix. Notations $\text{tr}(\mathbf{X})$, $\text{Rank}(\mathbf{X})$, and $\det(\mathbf{X})$ denote the matrix \mathbf{X} trace, rank, and determinant, respectively. Notation $\text{diag}(\mathbf{x})$ denotes a diagonal matrix whose diagonal elements are given by the vector \mathbf{x} . Notation $\mathbf{A} \circ \mathbf{B}$ denotes the Hadamard (element-wise) product. Notations $\mathbf{X}[m, n]$, $\mathbf{X}[m, :]$, and $\mathbf{X}[:, n]$ denote the m -th row and the n -th column element of matrix \mathbf{X} , the m -th row vector of matrix \mathbf{X} , and the n -th column vector of matrix \mathbf{X} , respectively.

II. SYSTEM MODEL

As illustrated in Fig. 1, this paper is concerned with the LISA-assisted SR system which consists of one BS with M antennas, one PR with N_1 antennas, one LISA with K reflecting elements, and one IR with N_2 antennas. Similar to [21]–[29], perfect CSI is assumed to be available at LISA, and the CSI acquisition techniques can be found in [30], [31]. In the following, we provide the channel model, the reflecting coefficient model, and the transmission model for the LISA-assisted SR system.

A. Channel Model

We consider the block flat-fading channel model, i.e., the channel coefficients remain unchanged during one block but may vary from one block to another. As shown in Fig. 1, denote by $\mathbf{H}_1 \in \mathbb{C}^{K \times M}$, $\mathbf{H}_2 \in \mathbb{C}^{N_2 \times M}$, $\mathbf{H}_3 \in \mathbb{C}^{N_1 \times M}$, $\mathbf{G}_1 \in \mathbb{C}^{N_1 \times K}$, and $\mathbf{G}_2 \in \mathbb{C}^{N_2 \times K}$ the baseband equivalent channel responses from BS to LISA, from BS to IR, from BS to PR, from LISA to PR, and LISA to IR, respectively. Each channel response consists of two components: a large-scale fading component and a small-scale fading component. Without loss of generality, the large-scale fading is distance-dependent and can be modeled as

$$\eta(d) = \frac{\beta}{d^{\gamma_e}}, \quad (1)$$

where d is the link distance from the transmitter to the receiver, β is the path loss at the reference distance of 1 meter (m), and γ_e is the path loss exponent. Denote by $d_{h,1}$ the distance from BS to LISA, by $d_{h,2}$ the distance from BS to IR, by $d_{h,3}$ the distance from BS to PR, by $d_{g,1}$ the distance from LISA to PR, and by $d_{g,2}$ the distance from LISA to IR.

Without loss of generality, the small-scale fading component of \mathbf{H}_1 is assumed to follow the Rician fading channel model, which consists of a *line of sight* (LoS) component and a *non-LoS* (NLoS) component, i.e.,

$$\mathbf{H}_1 = \sqrt{\eta(d_{h,1})} \left(\sqrt{\frac{\kappa}{\kappa+1}} \mathbf{H}_1^{\text{LoS}} + \sqrt{\frac{1}{\kappa+1}} \mathbf{H}_1^{\text{NLoS}} \right), \quad (2)$$

where κ is the Rician factor, $\mathbf{H}_1^{\text{LoS}}$ and $\mathbf{H}_1^{\text{NLoS}}$ are the LoS component and the NLoS component of \mathbf{H}_1 , respectively. Particularly, each element of $\mathbf{H}_1^{\text{NLoS}}$ follows the complex Gaussian distribution with zero mean and unit variance, while the LoS component can be expressed by the steering vector model, which is given by

$$\mathbf{H}_1^{\text{LoS}} = \mathbf{a}_K(\theta^{\text{AoA}}) \mathbf{a}_M^H(\theta^{\text{AoD}}), \quad (3)$$

where $\mathbf{a}_X(\theta) = \left[1, e^{j\frac{2\pi d_a}{\lambda} \sin \theta}, \dots, e^{j\frac{2\pi d_a}{\lambda} (X-1) \sin \theta} \right]^T$, $X = \{K, M\}$, d_a is the antenna spacing, λ is the wavelength, and θ^{AoA} and θ^{AoD} are the *angle of arrival* (AoA) at LISA and the *angle of departure* (AoD) at BS, respectively. The small-scale fading components of \mathbf{H}_2 , \mathbf{H}_3 , \mathbf{G}_1 , and \mathbf{G}_2 follow the Rayleigh fading channel model, in which each channel element follows the distribution of $\mathcal{CN}(0, 1)$.

B. Reflecting Coefficient Model

Let φ_k be the reflecting coefficient at the k -th element of LISA. Denote by \mathcal{A} the feasible set of the reflecting coefficients φ_k , for $k = 1, \dots, K$. In [32], only the phase can be continuously changed by loading each reflecting element with a varactor diode. Thus, in this paper, we consider that \mathcal{A} can be represented as

$$\mathcal{A} = \left\{ e^{j\phi} \mid \phi \in [0, 2\pi) \right\}. \quad (4)$$

C. Transmission Model

1) *Transmitted Signal at BS*: Denote by $\mathbf{s}(l)$ the $M \times 1$ symbol vector transmitted from BS to PR with $\mathbb{E}[\mathbf{s}(l)\mathbf{s}^H(l)] = \mathbf{I}_M$, and by $\mathbf{W} \in \mathbb{C}^{M \times M}$ the transmit beamforming matrix. Then the transmitted signal at BS can be written as $\mathbf{W}\mathbf{s}(l)$.

2) *Reflected Signal at LISA*: We assume that LISA applies a *binary phase shift keying* (BPSK) modulation scheme for IoT information transmission. Denote by c the message from LISA to IR, i.e., $c = \{1, -1\}$. Since the IoT transmission rate is much lower than the primary transmission rate, we assume each symbol period of c covers $L(L \gg 1)$ symbol periods of \mathbf{s} . The reflected signal from LISA can thus be expressed

as $\sqrt{\alpha}\Psi\mathbf{H}_1\mathbf{W}\mathbf{s}(l)c$, for $l = 1, \dots, L$, where $\Psi = \text{diag}(\varphi)$, $\varphi = [\varphi_1, \varphi_2, \dots, \varphi_K]^T$, and α denotes the reflection efficiency.

3) *Received Signal at PR*: In the l -th BS symbol period within one LISA symbol period of interest, the received signal at PR, $\mathbf{y}_p(l) \in \mathbb{C}^{N_1 \times 1}$ for $l = 1, \dots, L$, can be written as

$$\begin{aligned}\mathbf{y}_p(l) &= \mathbf{H}_3\mathbf{W}\mathbf{s}(l) + \sqrt{\alpha}\mathbf{G}_1\Psi\mathbf{H}_1\mathbf{W}\mathbf{s}(l)c + \mathbf{u}_p(l) \\ &= (\mathbf{H}_3 + \sqrt{\alpha}c\mathbf{G}_1\Psi\mathbf{H}_1)\mathbf{W}\mathbf{s}(l) + \mathbf{u}_p(l),\end{aligned}\quad (5)$$

where $\mathbf{u}_p(l) \in \mathbb{C}^{N_1 \times 1}$ is the complex Gaussian noise vector at PR that follows distribution $\mathcal{CN}(0, \sigma^2\mathbf{I}_{N_1})$. Since the symbol period of c is much larger than that of \mathbf{s} , the backscatter link can be treated as a multi-path component when decoding $\mathbf{s}(l)$ [11]. Thus, when decoding $\mathbf{s}(l)$, the signal-plus-noise covariance matrix is given by

$$\mathbf{\Gamma}_p = \frac{1}{\sigma^2}(\mathbf{H}_3 + \sqrt{\alpha}c\mathbf{G}_1\Psi\mathbf{H}_1)\mathbf{W}\mathbf{W}^H(\mathbf{H}_3 + \sqrt{\alpha}c\mathbf{G}_1\Psi\mathbf{H}_1)^H. \quad (6)$$

From (6), the expression of $\mathbf{\Gamma}_p$ contains c , which changes relatively fast as compared to the channel variation. Thus, according to [33], the achievable rate of the primary transmission needs to take expectation over c , which is given by

$$R_p = \mathbb{E}_c[\log_2 \det(\mathbf{I}_{N_1} + \mathbf{\Gamma}_p(c))]. \quad (7)$$

4) *Received Signal at IR*: For the LISA symbol period of interest, the received signal at IR, $\mathbf{y}_b(l) \in \mathbb{C}^{N_2 \times 1}$ for $l = 1, \dots, L$, can be written as

$$\mathbf{y}_b(l) = \mathbf{H}_2\mathbf{W}\mathbf{s}(l) + \sqrt{\alpha}\mathbf{G}_2\Psi\mathbf{H}_1\mathbf{W}\mathbf{s}(l)c + \mathbf{u}_b(l), \quad (8)$$

where $\mathbf{u}_b(l) \in \mathbb{C}^{N_2 \times 1}$ is the complex Gaussian noise vector at IR that follows distribution $\mathcal{CN}(0, \sigma^2\mathbf{I}_{N_2})$. Due to the coupling between $\mathbf{s}(l)$ and c in the second term in (8), we assume that IR decodes $\mathbf{s}(l)$ and c jointly based on *maximum likelihood* (ML) detection to achieve a better performance [9]. In that case, according Appendix A, the signal-plus-noise covariance matrix for decoding $\mathbf{s}(l)$ and the SNR for decoding c are respectively given by

$$\mathbf{\Gamma}_{b,s} = \frac{1}{\sigma^2}(\mathbf{H}_2 + \sqrt{\alpha}c\mathbf{G}_2\Psi\mathbf{H}_1)\mathbf{W}\mathbf{W}^H(\mathbf{H}_2 + \sqrt{\alpha}c\mathbf{G}_2\Psi\mathbf{H}_1)^H, \quad (9)$$

$$\gamma_{b,c} = \frac{\alpha L}{\sigma^2} \text{tr}(\mathbf{G}_2\Psi\mathbf{H}_1\mathbf{W}\mathbf{W}^H\mathbf{H}_1^H\Psi^H\mathbf{G}_2^H). \quad (10)$$

The achievable rate of $\mathbf{s}(l)$ from BS to IR is given by [11]

$$R_{b,s} = \mathbb{E}_c[\log_2 \det(\mathbf{I}_{N_2} + \mathbf{\Gamma}_{b,s}(c))]. \quad (11)$$

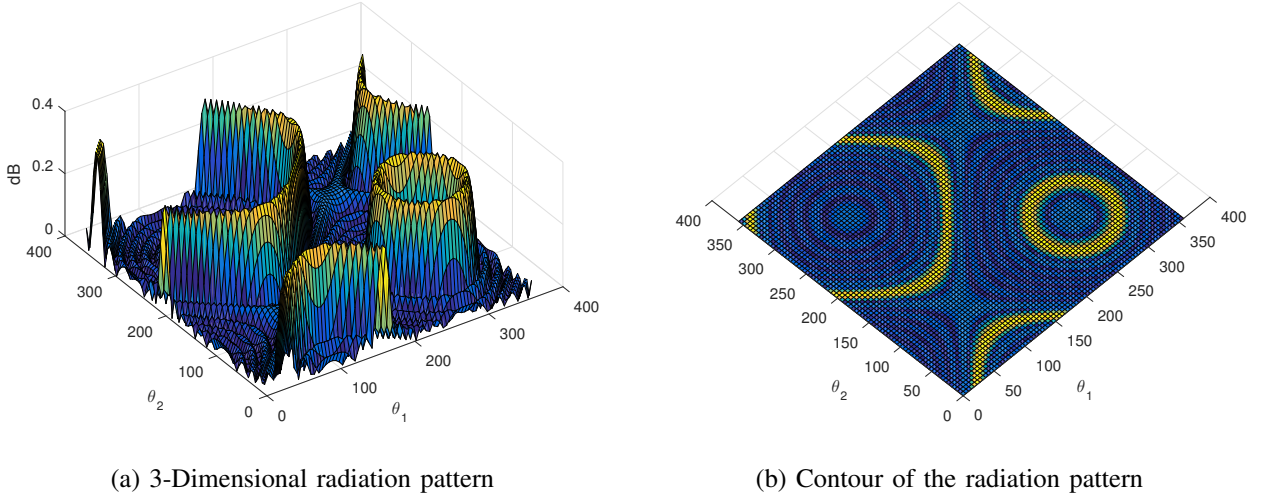


Fig. 2: Radiation pattern of LISA.

III. PRINCIPLES OF LISA FOR SR

The key feature of LISA is that the coefficients on each reflecting element can be adjusted such that the formed beams can be pointed to the desired directions. The reflecting process for LISA is performed on the RF level, and thus the reflected signal at each reflecting element is the multiplication of its reflecting coefficient, its received signal, and the transmitted message of LISA. Note that the noise at LISA is neglected since the reflecting process is executed on the ambient RF signals, which only involves passive components [34].

For convenience to capturing the beamforming effects of LISA, without loss of generality, we first consider the case with single antenna BS and single antenna IR. Redefine the channel response from BS to LISA as \mathbf{h} , and the channel response from LISA to IR as \mathbf{g} . We consider the simple steering vector channel model, i.e., $\mathbf{h} = [1, e^{j\frac{2\pi d_a}{\lambda} \sin \theta_1}, \dots, e^{j\frac{2\pi d_a(K-1)}{\lambda} \sin \theta_1}]^T$ and $\mathbf{g} = [1, e^{j\frac{2\pi d_a}{\lambda} \sin \theta_2}, \dots, e^{j\frac{2\pi d_a(K-1)}{\lambda} \sin \theta_2}]^T$, where θ_1 is the AoA from BS to LISA and θ_2 is the AoD from LISA to IR. The received backscatter signal at IR, y_b , can be rewritten as

$$y_b = \sqrt{\alpha} \mathbf{g}^H \mathbf{\Psi} \mathbf{h} s c, \quad (12)$$

where s represents the transmitted signal at BS. Since $\mathbf{g}^H \mathbf{\Psi} = \boldsymbol{\varphi}^T \text{diag}(\mathbf{g}^H)$, the received signal (12) at IR can be recast as

$$y_b = \sqrt{\alpha} \boldsymbol{\varphi}^T \text{diag}(\mathbf{g}^H) \mathbf{h} s c, \quad (13)$$

Substituting the channel responses \mathbf{h} and \mathbf{g} into (13), then we have

$$\text{diag}(\mathbf{g}^H) \mathbf{h} = [1, e^{j\frac{2\pi d_a}{\lambda} (\sin \theta_1 - \sin \theta_2)}, \dots, e^{j\frac{2\pi d_a(K-1)}{\lambda} (\sin \theta_1 - \sin \theta_2)}]^T. \quad (14)$$

By assuming $\varphi = [1, e^{j\frac{2\pi d_a}{\lambda} \sin \psi}, \dots, e^{j\frac{2\pi d_a}{\lambda} (K-1) \sin \psi}]^T$, according to Appendix B, when $\sin \psi + \sin \theta_1 - \sin \theta_2 = \frac{\ell \lambda}{d_a}$, the strength of the backscatter link signal is maximized, where $\ell \in \mathbf{Z}$ is an arbitrary integer. That means for a given ψ , provided that the AoD and the AoA at LISA satisfy the condition that $\sin \theta_2 - \sin \theta_1 = \sin \psi - \frac{\ell \lambda}{d_a}$, $\ell \in \mathbf{Z}$, LISA can maximally enhance the strength of the backscatter link signal. Furthermore, it is observed that for a given ψ , there exist multiple pairs of θ_1 and θ_2 satisfying $\sin \theta_2 - \sin \theta_1 = \sin \psi - \frac{\ell \lambda}{d_a}$, $\ell \in \mathbf{Z}$, which implies that LISA can enhance more than one transmission simultaneously. Fig. 2a and Fig. 2b show the 3-dimensional radiation pattern and the contour of the radiation pattern, respectively, which plot $|y_b|^2$ in (13) versus θ_1 and θ_2 with $\varphi_k = e^{-jk\pi \sin(\frac{\pi}{8})}$, for $k = 1, \dots, 8$. From Fig. 2, it is seen that for a given φ , LISA has different impacts on the different pairs of θ_1 and θ_2 . Specifically, we list some examples to demonstrate the beamforming effects of LISA as follows.

- For $\theta_2 = 90^\circ$, one backscatter link from the direction of $\theta_1 = 220^\circ$ is enhanced, while the link from the direction of $\theta_1 = 120^\circ$ is suppressed. That is to say, for one given receiver, LISA can enhance one link signal strength from one direction and simultaneously suppress the other link signal strength from the other direction.
- For two links with $\theta_1 = 90^\circ, \theta_2 = 150^\circ$ and $\theta_1 = 200^\circ, \theta_2 = 250^\circ$, the signal strength is enhanced simultaneously, which means that LISA can assist multiple link transmissions at the same time.
- By assuming that the AoA from BS to LISA is $\theta_1 = 90^\circ$, the AoD from LISA to IR is $\theta_2 = 50^\circ$, and the AoD from LISA to PR is 150° , it is observed that the strength of the received signals at both IR and PR is enhanced. That is, LISA will help to enhance the signals to both PR and IR from BS.

In summary, from Fig. 2, it is found that with proper reflecting beamforming design, LISA can assist multiple transmissions simultaneously, or assist one transmission while suppressing other transmissions. These insights indicate that LISA has many promising applications in SR systems which require the enhancement for both primary transmission and IoT communications. For the case with multiple antennas at BS and IR, similar effects can be expected with additional beamforming design at BS and IR.

IV. POWER MINIMIZATION FOR THE GENERAL CASE

Section III reveals the feasible effect of reflecting beamforming at LISA SR systems, i.e., with properly designed reflecting coefficients, LISA can not only enhance the primary transmission but also assist the IoT communication. In this section, we will jointly optimize the active transmit beamforming at BS and the passive reflecting beamforming at LISA to minimize the BS transmit power, subject to the rate constraint for the primary transmission and the SNR constraint for the IoT communication.

A. Problem Formulation

We aim to minimize the BS transmit power, subject to the rate constraint of the primary transmission and the SNR constraint of the IoT communication. Since IR decodes $s(l)$ and c jointly, $R_{b,s}$ needs to satisfy the rate constraint to guarantee that $s(l)$ and c can be jointly decoded successfully. Mathematically, the corresponding optimization problem can be formulated as

$$\mathbf{P1} : \min_{\mathbf{W}, \Psi} \text{tr}(\mathbf{W}\mathbf{W}^H) \quad (15a)$$

$$s.t. R_p \geq R_s, \quad (15a)$$

$$R_{b,s} \geq R_s, \quad (15b)$$

$$\gamma_{b,c} \geq \gamma, \quad (15c)$$

$$\varphi_k \in \mathcal{A}, \quad \forall k = 1, \dots, K, \quad (15d)$$

where R_s is the primary transmission rate, and γ is the required SNR at IR to support the IoT communication.

The active transmit beamformer \mathbf{W} and the passive reflecting beamformer Ψ are coupled together in the constraints of $\mathbf{P1}$, and thus the constraints (15a), (15b), and (15c) are not convex set. Also, the constraint on each reflecting coefficient φ_k is non-convex. Therefore, the problem $\mathbf{P1}$ is a non-convex optimization problem, resulting in the difficulty in solving it. Fortunately, the *alternating optimization* (AO) method is a widely exploited approach in tackling such non-convex matrix optimization problem [35], [36]. In the following, we will apply the AO method to solve the optimization problem $\mathbf{P1}$.

B. Optimization Algorithms

The main idea of the AO method is to iteratively solve a series of convex subproblems until convergence [24], [36]. The subproblem is the optimization problem with respect to one variable with all other variables being fixed. Specifically, the problem $\mathbf{P1}$ is decoupled into a series of subproblems with respect to one variable in $\{\mathbf{W}, \varphi_k, k = 1, \dots, K\}$, by fixing all other K variables, which are given by

$$\mathbf{P1} - \mathbf{a} : \min_{\mathbf{W}} \text{tr}(\mathbf{W}\mathbf{W}^H) \quad (15a)$$

$$s.t. (15a), (15b), \text{ and } (15c),$$

and

$$\mathbf{P1} - k : \min_{\varphi_k} \text{tr}(\mathbf{W}\mathbf{W}^H) \quad (15b)$$

$$s.t. (15a), (15b), (15c), \text{ and } (15d),$$

for $k = 1, \dots, K$. In the following, we will provide the solutions to the subproblems $\mathbf{P1} - \mathbf{a}$ and $\mathbf{P1} - k$.

1) *Solution to $\mathbf{P1} - \mathbf{a}$* : By introducing a new variable $\mathbf{Q} \triangleq \mathbf{W}\mathbf{W}^H$, $\mathbf{P1} - \mathbf{a}$ can be recast as the following equivalent problem:

$$\mathbf{P2} - \mathbf{a}: \min_{\mathbf{Q}} \text{tr}(\mathbf{Q})$$

$$s.t. f_1(\mathbf{Q}) \geq R_s, \quad (18a)$$

$$f_2(\mathbf{Q}) \geq R_s, \quad (18b)$$

$$\frac{L}{\sigma^2} \text{tr}(\mathbf{F}_2 \mathbf{Q} \mathbf{F}_2^H) \geq \gamma, \quad (18c)$$

where $f_1(\mathbf{Q}) \triangleq \mathbb{E}_c[\log_2 \det(\mathbf{I}_{N_1} + \frac{1}{\sigma^2}(\mathbf{H}_3 + \mathbf{F}_1 c) \mathbf{Q} (\mathbf{H}_3 + \mathbf{F}_1 c)^H)]$, $f_2(\mathbf{Q}) \triangleq \mathbb{E}_c[\log_2 \det(\mathbf{I}_{N_2} + \frac{1}{\sigma^2}(\mathbf{H}_2 + \mathbf{F}_2 c) \mathbf{Q} (\mathbf{H}_2 + \mathbf{F}_2 c)^H)]$, $\mathbf{F}_1 = \sqrt{\alpha} \mathbf{G}_1 \Psi \mathbf{H}_1$, and $\mathbf{F}_2 = \sqrt{\alpha} \mathbf{G}_2 \Psi \mathbf{H}_1$. Since the message c adopts BPSK modulation scheme, the expectation over c can be written as

$$f_1(\mathbf{Q}) = \frac{1}{2} \log_2 \det(\mathbf{I}_{N_1} + \frac{1}{\sigma^2}(\mathbf{H}_3 + \mathbf{F}_1) \mathbf{Q} (\mathbf{H}_3^H + \mathbf{F}_1^H)) + \frac{1}{2} \log_2 \det(\mathbf{I}_{N_1} + \frac{1}{\sigma^2}(\mathbf{H}_3 - \mathbf{F}_1) \mathbf{Q} (\mathbf{H}_3^H - \mathbf{F}_1^H)),$$

$$f_2(\mathbf{Q}) = \frac{1}{2} \log_2 \det(\mathbf{I}_{N_2} + \frac{1}{\sigma^2}(\mathbf{H}_2 + \mathbf{F}_2) \mathbf{Q} (\mathbf{H}_2^H + \mathbf{F}_2^H)) + \frac{1}{2} \log_2 \det(\mathbf{I}_{N_2} + \frac{1}{\sigma^2}(\mathbf{H}_2 - \mathbf{F}_2) \mathbf{Q} (\mathbf{H}_2^H - \mathbf{F}_2^H)).$$

Since $\log_2 \det(\cdot)$ is a concave function and \mathbf{Q} is positive semi-definite, the problem $\mathbf{P2} - \mathbf{a}$ is a standard convex *semi-definite program* (SDP) problem, Therefore, this problem can be efficiently solved by using the existing tools, such as CVX [37]. After deriving the optimal \mathbf{Q}^* , *singular value decomposition* (SVD) is used to obtain \mathbf{W} . Specifically, we first compute the SVD of \mathbf{Q}^* as $\mathbf{Q}^* = \mathbf{U} \Sigma \mathbf{U}^H$, where $\mathbf{U} \in \mathbb{C}^{M \times M}$ is a unitary matrix and Σ is an $M \times M$ diagonal matrix whose diagonal elements are the singular value of \mathbf{Q}^* . Since $\mathbf{Q}^* = \mathbf{W}^* (\mathbf{W}^*)^H$, we have $\mathbf{W}^* = \mathbf{U} \Sigma^{1/2}$.

2) *Solution to $\mathbf{P1} - k$* : Since the optimization variable φ_k in problem $\mathbf{P1} - k$ is implicit, we need to rewrite the constraints (15a), (15b), and (15c), and provide more tractable expressions for the problem $\mathbf{P1} - k$. To begin with, we rewrite \mathbf{F}_1 and \mathbf{F}_2 as $\mathbf{F}_1 = \sqrt{\alpha} \mathbf{G}_1 \Psi \mathbf{H}_1 = \sqrt{\alpha} \sum_{k=1}^K \varphi_k \mathbf{g}_{1,k} \mathbf{h}_{1,k}^H$ and $\mathbf{F}_2 = \sqrt{\alpha} \mathbf{G}_2 \Psi \mathbf{H}_1 = \sqrt{\alpha} \sum_{k=1}^K \varphi_k \mathbf{g}_{2,k} \mathbf{h}_{1,k}^H$, respectively, where $\mathbf{g}_{1,k} \in \mathbb{C}^{N_1 \times 1}$ is the k -th column vector of \mathbf{G}_1 , $\mathbf{h}_{1,k} \in \mathbb{C}^{M \times 1}$ is the k -th column vector of \mathbf{H}_1^H , and $\mathbf{g}_{2,k} \in \mathbb{C}^{N_2 \times 1}$ is the k -th column vector of \mathbf{G}_2 . Then the simplified constraints (15a), (15b), and (15c) are given in the following theorem.

Theorem 1. The simplified constraints (15a), (15b), and (15c) can be written as

$$f_3(\varphi_k) + f_4(\varphi_k) \geq 2R_s, \quad (19)$$

$$f_5(\varphi_k) + f_6(\varphi_k) \geq 2R_s, \quad (20)$$

$$f_7(\varphi_k) \geq \gamma, \quad (21)$$

where

$$f_3(\varphi_k) \triangleq \log_2 \det(\mathbf{I}_{N_1} + \frac{1}{\sigma^2}(\mathbf{H}_3 + \mathbf{F}_1) \mathbf{Q} (\mathbf{H}_3 + \mathbf{F}_1)^H)$$

$$= \begin{cases} \log_2 \det(\mathbf{A}_{1,k}), & \text{if } \text{rank}(\mathbf{A}_{1,k}^{-1} \mathbf{B}_{1,k}) = 0, \\ \log_2 \det(\mathbf{A}_{1,k} - \mathbf{B}_{1,k}^H \mathbf{A}_{1,k}^{-1} \mathbf{B}_{1,k}), & \text{if } \text{rank}(\mathbf{A}_{1,k}^{-1} \mathbf{B}_{1,k}) = 1, \text{tr}(\mathbf{A}_{1,k}^{-1} \mathbf{B}_{1,k}) = 0, \\ \log_2 (1 + |\lambda_{1,k}|^2 (1 - \tilde{v}_{1,k} v_{1,k}) + 2\text{Re}(\varphi_k \lambda_{1,k})) + \log_2 \det(\mathbf{A}_{1,k}), & \text{otherwise,} \end{cases}$$

$$f_4(\varphi_k) \triangleq \log_2 \det(\mathbf{I}_{N_1} + \frac{1}{\sigma^2} (\mathbf{H}_3 - \mathbf{F}_1) \mathbf{Q} (\mathbf{H}_3 - \mathbf{F}_1)^H)$$

$$= \begin{cases} \log_2 \det(\mathbf{A}_{2,k}), & \text{if } \text{rank}(\mathbf{A}_{2,k}^{-1} \mathbf{B}_{2,k}) = 0, \\ \log_2 \det(\mathbf{A}_{2,k} - \mathbf{B}_{2,k}^H \mathbf{A}_{2,k}^{-1} \mathbf{B}_{2,k}), & \text{if } \text{rank}(\mathbf{A}_{2,k}^{-1} \mathbf{B}_{2,k}) = 1, \text{tr}(\mathbf{A}_{2,k}^{-1} \mathbf{B}_{2,k}) = 0, \\ \log_2 (1 + |\lambda_{2,k}|^2 (1 - \tilde{v}_{2,k} v_{2,k}) + 2\text{Re}(\varphi_k \lambda_{2,k})) + \log_2 \det(\mathbf{A}_{2,k}), & \text{otherwise,} \end{cases}$$

$$f_5(\varphi_k) \triangleq \log_2 \det(\mathbf{I}_{N_2} + \frac{1}{\sigma^2} (\mathbf{H}_2 + \mathbf{F}_2) \mathbf{Q} (\mathbf{H}_2 + \mathbf{F}_2)^H)$$

$$= \begin{cases} \log_2 \det(\mathbf{A}_{3,k}), & \text{if } \text{rank}(\mathbf{A}_{3,k}^{-1} \mathbf{B}_{3,k}) = 0, \\ \log_2 \det(\mathbf{A}_{3,k} - \mathbf{B}_{3,k}^H \mathbf{A}_{3,k}^{-1} \mathbf{B}_{3,k}), & \text{if } \text{rank}(\mathbf{A}_{3,k}^{-1} \mathbf{B}_{3,k}) = 1, \text{tr}(\mathbf{A}_{3,k}^{-1} \mathbf{B}_{3,k}) = 0, \\ \log_2 (1 + |\lambda_{3,k}|^2 (1 - \tilde{v}_{3,k} v_{3,k}) + 2\text{Re}(\varphi_k \lambda_{3,k})) + \log_2 \det(\mathbf{A}_{3,k}), & \text{otherwise,} \end{cases}$$

$$f_6(\varphi_k) \triangleq \log_2 \det(\mathbf{I}_{N_2} + \frac{1}{\sigma^2} (\mathbf{H}_2 - \mathbf{F}_2) \mathbf{Q} (\mathbf{H}_2 - \mathbf{F}_2)^H)$$

$$= \begin{cases} \log_2 \det(\mathbf{A}_{4,k}), & \text{if } \text{rank}(\mathbf{A}_{4,k}^{-1} \mathbf{B}_{4,k}) = 0, \\ \log_2 \det(\mathbf{A}_{4,k} - \mathbf{B}_{4,k}^H \mathbf{A}_{4,k}^{-1} \mathbf{B}_{4,k}), & \text{if } \text{rank}(\mathbf{A}_{4,k}^{-1} \mathbf{B}_{4,k}) = 1, \text{tr}(\mathbf{A}_{4,k}^{-1} \mathbf{B}_{4,k}) = 0, \\ \log_2 (1 + |\lambda_{4,k}|^2 (1 - \tilde{v}_{4,k} v_{4,k}) + 2\text{Re}(\varphi_k \lambda_{4,k})) + \log_2 \det(\mathbf{A}_{4,k}), & \text{otherwise,} \end{cases}$$

$$f_7(\varphi_k) \triangleq \frac{L}{\sigma^2} \text{tr}(\mathbf{F}_2 \mathbf{Q} \mathbf{F}_2^H) = \frac{\alpha L}{\sigma^2} (A_{5,k} + 2\text{Re}(\varphi_k B_{5,k})),$$

where $\mathbf{A}_{1,k} \triangleq \mathbf{I}_{N_1} + \frac{1}{\sigma^2} \mathbf{H}_3 \mathbf{Q} \mathbf{H}_3^H + \frac{\alpha}{\sigma^2} \mathbf{g}_{1,k} \mathbf{h}_{1,k}^H \mathbf{Q} \mathbf{h}_{1,k} \mathbf{g}_{1,k}^H + \frac{\sqrt{\alpha}}{\sigma^2} \sum_{i \neq k} (\varphi_i \mathbf{g}_{1,i} \mathbf{h}_{1,i}^H \mathbf{Q} \mathbf{H}_3^H + \varphi_i^\dagger \mathbf{H}_3 \mathbf{Q} \mathbf{h}_{1,i} \mathbf{g}_{1,i}^H) + \frac{\alpha}{\sigma^2} (\sum_{i \neq k} \varphi_i \mathbf{g}_{1,i} \mathbf{h}_{1,i}^H) \mathbf{Q} (\sum_{i \neq k} \varphi_i^\dagger \mathbf{h}_{1,i} \mathbf{g}_{1,i}^H)$, $\mathbf{B}_{1,k} \triangleq \frac{\sqrt{\alpha}}{\sigma^2} \mathbf{g}_{1,k} \mathbf{h}_{1,k}^H \mathbf{Q} \mathbf{H}_3^H + \frac{\alpha}{\sigma^2} \sum_{i \neq k} \varphi_i^\dagger \mathbf{g}_{1,k} \mathbf{h}_{1,k}^H \mathbf{Q} \mathbf{h}_{1,i} \mathbf{g}_{1,i}^H$, $\mathbf{A}_{2,k} \triangleq \mathbf{I}_{N_1} + \frac{1}{\sigma^2} \mathbf{H}_3 \mathbf{Q} \mathbf{H}_3^H + \frac{\alpha}{\sigma^2} \mathbf{g}_{1,k} \mathbf{h}_{1,k}^H \mathbf{Q} \mathbf{h}_{1,k} \mathbf{g}_{1,k}^H - \frac{\sqrt{\alpha}}{\sigma^2} \sum_{i \neq k} (\varphi_i \mathbf{g}_{1,i} \mathbf{h}_{1,i}^H \mathbf{Q} \mathbf{H}_3^H + \varphi_i^\dagger \mathbf{H}_3 \mathbf{Q} \mathbf{h}_{1,i} \mathbf{g}_{1,i}^H) + \frac{\alpha}{\sigma^2} (\sum_{i \neq k} \varphi_i \mathbf{g}_{1,i} \mathbf{h}_{1,i}^H) \mathbf{Q} (\sum_{i \neq k} \varphi_i^\dagger \mathbf{h}_{1,i} \mathbf{g}_{1,i}^H)$, $\mathbf{B}_{2,k} \triangleq -\frac{\sqrt{\alpha}}{\sigma^2} \mathbf{g}_{1,k} \mathbf{h}_{1,k}^H \mathbf{Q} \mathbf{H}_3^H + \frac{\alpha}{\sigma^2} \sum_{i \neq k} \varphi_i^\dagger \mathbf{g}_{1,k} \mathbf{h}_{1,k}^H \mathbf{Q} \mathbf{h}_{1,i} \mathbf{g}_{1,i}^H$, $\mathbf{A}_{3,k} \triangleq \mathbf{I}_{N_2} + \frac{1}{\sigma^2} \mathbf{H}_2 \mathbf{Q} \mathbf{H}_2^H + \frac{\alpha}{\sigma^2} \mathbf{g}_{2,k} \mathbf{h}_{1,k}^H \mathbf{Q} \mathbf{h}_{1,k} \mathbf{g}_{2,k}^H + \frac{\sqrt{\alpha}}{\sigma^2} \sum_{i \neq k} (\varphi_i \mathbf{g}_{2,i} \mathbf{h}_{1,i}^H \mathbf{Q} \mathbf{H}_2^H + \varphi_i^\dagger \mathbf{H}_2 \mathbf{Q} \mathbf{h}_{1,i} \mathbf{g}_{2,i}^H) + \frac{\alpha}{\sigma^2} (\sum_{i \neq k} \varphi_i \mathbf{g}_{2,i} \mathbf{h}_{1,i}^H) \mathbf{Q} (\sum_{i \neq k} \varphi_i^\dagger \mathbf{h}_{1,i} \mathbf{g}_{2,i}^H)$, $\mathbf{B}_{3,k} \triangleq \frac{\sqrt{\alpha}}{\sigma^2} \mathbf{g}_{2,k} \mathbf{h}_{1,k}^H \mathbf{Q} \mathbf{H}_2^H + \frac{\alpha}{\sigma^2} \sum_{i \neq k} \varphi_i^\dagger \mathbf{g}_{2,k} \mathbf{h}_{1,k}^H \mathbf{Q} \mathbf{h}_{1,i} \mathbf{g}_{2,i}^H$, $\mathbf{A}_{4,k} \triangleq \mathbf{I}_{N_2} + \frac{1}{\sigma^2} \mathbf{H}_2 \mathbf{Q} \mathbf{H}_2^H + \frac{\alpha}{\sigma^2} \mathbf{g}_{2,k} \mathbf{h}_{1,k}^H \mathbf{Q} \mathbf{h}_{1,k} \mathbf{g}_{2,k}^H - \frac{\sqrt{\alpha}}{\sigma^2} \sum_{i \neq k} (\varphi_i \mathbf{g}_{2,i} \mathbf{h}_{1,i}^H \mathbf{Q} \mathbf{H}_2^H + \varphi_i^\dagger \mathbf{H}_2 \mathbf{Q} \mathbf{h}_{1,i} \mathbf{g}_{2,i}^H) + \frac{\alpha}{\sigma^2} (\sum_{i \neq k} \varphi_i \mathbf{g}_{2,i} \mathbf{h}_{1,i}^H) \mathbf{Q} (\sum_{i \neq k} \varphi_i^\dagger \mathbf{h}_{1,i} \mathbf{g}_{2,i}^H)$, $\mathbf{B}_{4,k} \triangleq -\frac{\sqrt{\alpha}}{\sigma^2} \mathbf{g}_{2,k} \mathbf{h}_{1,k}^H \mathbf{Q} \mathbf{H}_2^H + \frac{\alpha}{\sigma^2} \sum_{i \neq k} \varphi_i^\dagger \mathbf{g}_{2,k} \mathbf{h}_{1,k}^H \mathbf{Q} \mathbf{h}_{1,i} \mathbf{g}_{2,i}^H$, $A_{5,k} \triangleq \mathbf{g}_{2,k}^H \mathbf{g}_{2,k} \mathbf{h}_{1,k}^H \mathbf{Q} \mathbf{h}_{1,k} + \sum_{i_1 \neq k} \sum_{i_2 \neq k} \varphi_{i_1} \varphi_{i_2}^\dagger \mathbf{g}_{2,i_2}^H \mathbf{g}_{2,i_1} \mathbf{h}_{1,i_1}^H \mathbf{Q} \mathbf{h}_{1,i_2}$, and $B_{5,k} \triangleq \sum_{i \neq k} \varphi_i^\dagger \mathbf{g}_{2,i}^H \mathbf{g}_{2,k} \mathbf{h}_{1,k}^H \mathbf{Q} \mathbf{h}_{1,i}$. In addition, $\lambda_{i,k}$ is the non-zero eigenvalues of the matrix $\mathbf{A}_{i,k}^{-1} \mathbf{B}_{i,k}$, and $v_{i,k}$ and $\tilde{v}_{i,k}$ are the first elements of $(\mathbf{U}_{i,k}^H \mathbf{A}_{i,k} \mathbf{U}_{i,k})^{-1}$ and $\mathbf{U}_{i,k}^H \mathbf{A}_{i,k} \mathbf{U}_{i,k}$, respectively, where $\mathbf{U}_{i,k}$ is obtained from the eigendecomposition of matrix $\mathbf{A}_{i,k}^{-1} \mathbf{B}_{i,k}$ and $i \in \{1, 2, 3, 4\}$.

Proof: The details are given in Appendix C. ■

Based on the above theorem, the optimization problem can be recast as

$$\begin{aligned}
\mathbf{P2}-k : & \min_{\varphi_k} \text{tr}(\mathbf{Q}) \\
& \text{s.t. (19), (20), (21),} \\
& \varphi_k \in \mathcal{A}.
\end{aligned} \tag{22a}$$

For $\mathbf{P2}-k$, the objective function does not involve the variable φ_k which only exists in the constraints. It means that solving $\mathbf{P2}-k$ only obtains a feasible solution. In that case, it remains unknown whether the transmit power $\text{tr}(\mathbf{Q})$ will monotonically decrease or not, which will affect the convergence performance of $\mathbf{P1}$. Intuitively, if the feasible solution φ_k obtained by solving $\mathbf{P2}-k$ achieves a higher primary transmission rate than the required rate and a higher IoT transmission SNR than the required SNR, the minimum transmit power in $\mathbf{P2}-a$ can be reduced without violating all the constraints. To achieve it, we aim to maximize the minimum ratio of the primary transmission rate to its required rate and the IoT transmission SNR to its required SNR. More specifically, $\mathbf{P2}-k$ is transformed into the problem $\mathbf{P3}-k$:

$$\begin{aligned}
\mathbf{P3}-k : & \max_{\varphi_k} \min \left\{ \frac{f_3(\varphi_k) + f_4(\varphi_k)}{2R_s}, \frac{f_5(\varphi_k) + f_6(\varphi_k)}{2R_s}, \frac{f_7(\varphi_k)}{\gamma} \right\} \\
& \text{s.t. } \frac{f_3(\varphi_k) + f_4(\varphi_k)}{2R_s} \geq 1,
\end{aligned} \tag{23a}$$

$$\frac{f_5(\varphi_k) + f_6(\varphi_k)}{2R_s} \geq 1, \tag{23b}$$

$$\frac{f_7(\varphi_k)}{\gamma} \geq 1, \tag{23c}$$

$$\varphi_k \in \mathcal{A}, \quad \forall k = 1, \dots, K. \tag{23d}$$

By introducing a slack variable, according to [38], $\mathbf{P3}-k$ can be recast as the following problem:

$$\begin{aligned}
\mathbf{P3}-k1 : & \max_{\varphi_k, t} t \\
& \text{s.t. } \frac{f_3(\varphi_k) + f_4(\varphi_k)}{2R_s} \geq t,
\end{aligned} \tag{24a}$$

$$\frac{f_5(\varphi_k) + f_6(\varphi_k)}{2R_s} \geq t, \tag{24b}$$

$$\frac{f_7(\varphi_k)}{\gamma} \geq t, \tag{24c}$$

$$t \geq 1, \tag{24d}$$

$$\varphi_k \in \mathcal{A}. \tag{24e}$$

The constraint (24d) aims to guarantee that the problem $\mathbf{P3}-k1$ and problem $\mathbf{P2}-k$ have the same feasible set of φ_k . One can see that the constraint (24e) in problem $\mathbf{P3}-k1$ is not a convex set. To overcome this

challenge, we relax the constraint (24e) as $|\varphi_k|^2 \leq 1$, and then we solve the problem **P3**– $k1$ with $|\varphi_k|^2 \leq 1$, which is a convex problem, and thus can be solved optimally and effectively by *KarushKuhnTucker* (KKT) conditions. After that, we apply the projection method to obtain the solution to **P3**– $k1$ with $\varphi_k \in \mathcal{A}$. Specifically, we project the solution to **P3**– $k1$ with $|\varphi_k|^2 \leq 1$ into the set of $\varphi_k \in \mathcal{A}$. Denote by φ_k^* the optimal solution to the problem **P3**– $k1$ with $|\varphi_k|^2 \leq 1$. Then, the solution φ_k^* to the problem **P3**– $k1$ with $\varphi_k \in \mathcal{A}$ can be obtained by solving the following projection problem:

$$\begin{aligned} \mathbf{P4}\text{--}k : \quad & \max_{\varphi_k^*} \|\varphi_k^* - \varphi_k^*\|^2 \\ & s.t. \quad \varphi_k^* \in \mathcal{A}. \end{aligned}$$

The optimal solution to the above optimization problem **P4**– k is given by

$$\varphi_k^* = \exp(j \arg(\varphi_k^*)). \quad (26)$$

Note that the φ_k^* obtained by the projection method is not an optimum solution to the original non-convex problem **P3**– $k1$. Thus, we only update φ_k^* when all the constraints in **P3**– $k1$ are satisfied to guarantee the convergence performance. In addition, **P3**– $k1$ is more efficient than the problem **P2**– k concerning the convergence since the solution to **P3**– $k1$ achieves a strictly higher primary transmission rate and a strictly higher IoT transmission SNR, which can reduce the minimum transmit power.

C. Overall Algorithm for Solving **P1**

In this section, we present a detailed description of the proposed algorithm for solving **P1** based on the above analysis. Specifically, we first randomly generate I sets of $\{\varphi_k\}_{k=1}^K$ that satisfy $\varphi_k \in \mathcal{A}$. For each generated set of $\{\varphi_k\}_{k=1}^K$, we calculate the minimum transmit power by solving **P2** – a. Then, we select the set with minimum transmit power among all sets as the initial point $\{\varphi_k^0\}_{k=1}^K$. With the initial point, we iteratively solve **P2** – a and **P3**– $k1$ until convergence. The details of the algorithm steps to solve **P1** based on the AO method are summarized in Algorithm 1. In the following, we will analyze the convergence and computational complexity for solving **P1**.

D. Convergence and Complexity Analysis

1) *Convergence Analysis*: The convergence performance of the proposed algorithm is given in the following theorem.

Theorem 2. The value of the objective function decreases in each iteration of the proposed algorithm, i.e., $\text{tr}(\mathbf{Q}^{(t)}; \varphi^{(t)}) \leq \text{tr}(\mathbf{Q}^{(t-1)}; \varphi^{(t-1)})$.

Proof: The solution $\varphi_k^{(t)}$ to **P3**– $k1$ is in the feasible set of **P2**– k . Since the solution $\varphi_k^{(t)}$ by solving problem **P3**– $k1$ achieves a higher primary transmission rate and (or) a higher IoT transmission SNR, the

Algorithm 1 Solution to P1

- 1: Randomly generate I independent sets of $\{\varphi_k\}_{k=1}^K$ that satisfy $\varphi_k \in \mathcal{A}$ and calculate the minimum transmit power by solving **P2 – a**,
 - 2: Select the set $\{\tilde{\varphi}_k^*\}_{k=1}^K$ with minimum transmit power $\text{tr}(\tilde{\mathbf{Q}}^*)$ among all I sets as the initial point;
 - 3: Initialize $\mathbf{Q}^{(0)} = \tilde{\mathbf{Q}}^*$, $\{\varphi_k^{(0)}\}_{k=1}^K = \{\tilde{\varphi}_k^*\}_{k=1}^K$, and $t = 0$;
 - 4: **Repeat**
 - 5: $t \leftarrow t + 1$
 - 6: **for** $k = 1 \rightarrow K$
 - 7: Calculate $\varphi_k^{(t)}$ by solving **P3–k1** based on $\mathbf{Q}^{(t-1)}$, $\{\varphi_i^{(t)}\}_{i < k}$, and $\{\varphi_i^{(t-1)}\}_{i > k}$;
 - 8: **end**
 - 9: Calculate $\mathbf{Q}^{(t)}$ by solving **P2 – a** based on $\varphi^{(t)}$;
 - 10: **Until** the objective function of **P1** converges.
 - 11: Obtain \mathbf{W}^* based on SVD method.
-

minimum transmit power $\text{tr}(\mathbf{Q}^{(t)}; \varphi^{(t)})$ can be reduced in the t -th iteration until convergence. Mathematically, we have the following results:

$$\text{tr}(\mathbf{Q}^{(t-1)}; \varphi^{(t-1)}) \stackrel{(a)}{=} \text{tr}(\mathbf{Q}^{(t-1)}; \varphi^{(t)}) \stackrel{(b)}{\geq} \min_{\mathbf{Q}} \text{tr}(\mathbf{Q}; \varphi^{(t)}) = \text{tr}(\mathbf{Q}^{(t)}; \varphi^{(t)}), \quad (27)$$

where (a) holds since the transmit power only depends on \mathbf{Q} , and (b) holds since **P2 – a** is a convex problem. Hence, the convergence performance of the proposed algorithm can be guaranteed. ■

2) *Computational Complexity*: Here, we analyze the computational complexity of the proposed algorithm. According to [39], the computational complexity for solving **P2 – a** is $\mathcal{O}(M^2N_1^2 + MN_1^3 + M^2N_2^2 + MN_2^3)$ by using the path-following method for solving SDP. The computational complexity for solving **P3–k1** is $\mathcal{O}(N_1^3 + N_2^3)$ mainly caused by the matrix inversion and eigendecomposition. By assuming that the number of required iterations is $\mathcal{O}(J)$, the total computational complexity of the proposed algorithm is $\mathcal{O}(J(M^2N_1^2 + MN_1^3 + M^2N_2^2 + MN_2^3 + KN_1^3 + KN_2^3))$.

V. POWER MINIMIZATION FOR THE SPECIAL CASE

In this section, we consider the special case that the direct links signal is blocked, i.e., the received signals at IR and PR only involve the backscatter link signals. In that case, the formulated problem based on the problem **P1** can be rewritten as

$$\mathbf{P} - \mathbf{S} : \min_{\mathbf{Q}, \Psi} \text{tr}(\mathbf{Q})$$

$$s.t. \quad \log_2 \det(\mathbf{I}_{N_1} + \frac{1}{\sigma^2} \mathbf{F}_1 \mathbf{Q} \mathbf{F}_1^H) \geq R_s, \quad (28a)$$

$$\log_2 \det(\mathbf{I}_{N_2} + \frac{1}{\sigma^2} \mathbf{F}_2 \mathbf{Q} \mathbf{F}_2^H) \geq R_s, \quad (28b)$$

$$\frac{L}{\sigma^2} \text{tr}(\mathbf{F}_2 \mathbf{Q} \mathbf{F}_2^H) \geq \gamma, \quad (28c)$$

$$\varphi_k \in \mathcal{A}, \quad \forall k = 1, \dots, K. \quad (28d)$$

Based on the AO algorithm, $\mathbf{P} - \mathbf{S}$ can be decoupled into the following two subproblems with respect to \mathbf{Q} and Ψ , respectively:

$$\begin{aligned} \mathbf{P} - \mathbf{S1} : \quad & \min_{\mathbf{Q}} \text{tr}(\mathbf{Q}) \\ & \text{s.t. (28a), (28b), and (28c),} \end{aligned}$$

and

$$\begin{aligned} \mathbf{P} - \mathbf{S2} : \quad & \min_{\Psi} \text{tr}(\mathbf{Q}) \\ & \text{s.t. (28a), (28b), (28c), and (28d).} \end{aligned}$$

The problem $\mathbf{P} - \mathbf{S1}$ is a standard SDP problem, which can be efficiently solved by using the existing tools CVX. In the following, we focus on the solution to $\mathbf{P} - \mathbf{S2}$.

A. Solution to $\mathbf{P} - \mathbf{S2}$

We first simplify the constraints in the problem $\mathbf{P} - \mathbf{S2}$. Constraint (28a) can be written as

$$\begin{aligned} \log_2 \det(\mathbf{I}_{N_1} + \frac{1}{\sigma^2} \mathbf{F}_1 \mathbf{Q} \mathbf{F}_1^H) &\stackrel{(a)}{=} \log_2 \det(\mathbf{I}_M + \frac{1}{\sigma^2} \mathbf{F}_1^H \mathbf{F}_1 \mathbf{Q}) = \log_2 \det(\mathbf{I}_M + \frac{\alpha}{\sigma^2} \mathbf{H}_1^H \Psi^H \mathbf{G}_1^H \mathbf{G}_1 \Psi \mathbf{H}_1 \mathbf{Q}) \\ &\stackrel{(b)}{=} \log_2 \det(\mathbf{I}_M + \frac{\alpha}{\sigma^2} \mathbf{H}_1^H ((\mathbf{G}_1^H \mathbf{G}_1) \circ (\varphi^\dagger \varphi^T)) \mathbf{H}_1 \mathbf{Q}), \end{aligned} \quad (31)$$

where (a) is based on the property of $\det(\mathbf{I}_n + \mathbf{A}\mathbf{B}) = \det(\mathbf{I}_m + \mathbf{B}\mathbf{A})$ and (b) is based on the property of $\text{diag}(\mathbf{x})\mathbf{A}\text{diag}(\mathbf{y}^H) = \mathbf{A} \circ (\mathbf{x}\mathbf{y}^H)$. Similarly, we have

$$\log_2 \det(\mathbf{I}_{N_2} + \frac{1}{\sigma^2} \mathbf{F}_2 \mathbf{Q} \mathbf{F}_2^H) = \log_2 \det(\mathbf{I}_M + \frac{\alpha}{\sigma^2} \mathbf{H}_1^H ((\mathbf{G}_2^H \mathbf{G}_2) \circ (\varphi^\dagger \varphi^T)) \mathbf{H}_1 \mathbf{Q}). \quad (32)$$

For (28c), similarly, we have:

$$\text{tr}(\mathbf{F}_2 \mathbf{Q} \mathbf{F}_2^H) = \text{tr}(\mathbf{F}_2^H \mathbf{F}_2 \mathbf{Q}) = \alpha \text{tr}(\mathbf{H}_1^H \Psi^H \mathbf{G}_2^H \mathbf{G}_2 \Psi \mathbf{H}_1 \mathbf{Q}) = \alpha \text{tr}(\mathbf{H}_1^H ((\mathbf{G}_2^H \mathbf{G}_2) \circ (\varphi^\dagger \varphi^T)) \mathbf{H}_1 \mathbf{Q}). \quad (33)$$

By integrating (31), (32), and (33), we rewrite $\mathbf{P} - \mathbf{S2}$ as the following problem:

$$\begin{aligned} \mathbf{P} - \mathbf{S3} : \quad & \min_{\varphi} \text{tr}(\mathbf{Q}) \\ \text{s.t.} \quad & \log_2 \det(\mathbf{I}_M + \frac{\alpha}{\sigma^2} \mathbf{H}_1^H ((\mathbf{G}_1^H \mathbf{G}_1) \circ (\varphi^\dagger \varphi^T)) \mathbf{H}_1 \mathbf{Q}) \geq R_s, \quad (34a) \\ & \log_2 \det(\mathbf{I}_M + \frac{\alpha}{\sigma^2} \mathbf{H}_1^H ((\mathbf{G}_2^H \mathbf{G}_2) \circ (\varphi^\dagger \varphi^T)) \mathbf{H}_1 \mathbf{Q}) \geq R_s, \quad (34b) \\ & \frac{\alpha L}{\sigma^2} \text{tr}(\mathbf{H}_1^H ((\mathbf{G}_2^H \mathbf{G}_2) \circ (\varphi^\dagger \varphi^T)) \mathbf{H}_1 \mathbf{Q}) \geq \gamma, \quad (34c) \\ & \varphi_k \in \mathcal{A}, \quad \forall k = 1, \dots, K. \quad (34d) \end{aligned}$$

One can see that the constraints are not convex set, and thus the problem $\mathbf{P} - \mathbf{S3}$ is a non-convex optimization problem. The problem $\mathbf{P} - \mathbf{S3}$ can be seen as a generalized *quadratically constrained quadratic*

program (QCQP) optimization problem, which is an NP-hard problem. For solving $\mathbf{P} - \mathbf{S3}$, we have the following analysis.

By introducing a new variable $\Phi \triangleq \varphi^\dagger \varphi^T$, $\mathbf{P} - \mathbf{S3}$ can be recast as the following equivalent optimization problem:

$$\mathbf{P} - \mathbf{S4} : \min_{\Phi} \text{tr}(\mathbf{Q})$$

$$s.t. \quad \log_2 \det(\mathbf{I}_M + \frac{\alpha}{\sigma^2} \mathbf{H}_1^H ((\mathbf{G}_1^H \mathbf{G}_1) \circ \Phi) \mathbf{H}_1 \mathbf{Q}) \geq R_s, \quad (35a)$$

$$\log_2 \det(\mathbf{I}_M + \frac{\alpha}{\sigma^2} \mathbf{H}_1^H ((\mathbf{G}_2^H \mathbf{G}_2) \circ \Phi) \mathbf{H}_1 \mathbf{Q}) \geq R_s, \quad (35b)$$

$$\frac{\alpha L}{\sigma^2} \text{tr}(\mathbf{H}_1^H ((\mathbf{G}_2^H \mathbf{G}_2) \circ \Phi) \mathbf{H}_1 \mathbf{Q}) \geq \gamma, \quad (35c)$$

$$\text{Rank}(\Phi) = 1, \quad (35d)$$

$$\Phi[k, k] = 1, \quad \forall k = 1, \dots, K. \quad (35e)$$

In the problem $\mathbf{P} - \mathbf{S4}$, the rank-one constraint in (35d) is required since the variable $\Phi = \varphi^\dagger \varphi^T$ is a rank-one matrix. However, the rank-one constraint is non-convex, and thus we relax this constraint by applying SDR and have the following optimization problem:

$$\mathbf{P} - \mathbf{S5} : \min_{\Phi} \text{tr}(\mathbf{Q})$$

$$s.t. \quad (35a), (35b), (35c) \text{ and } (35e)$$

Similar to $\mathbf{P2-k}$, solving $\mathbf{P} - \mathbf{S5}$ only obtains a feasible solution. To accelerate the convergence for solving $\mathbf{P} - \mathbf{S}$, similar to section IV-B2, we transform $\mathbf{P} - \mathbf{S5}$ into the following optimization problem:

$$\mathbf{P} - \mathbf{S6} : \max_{\Phi, t} t$$

$$s.t. \quad \frac{1}{R_s} \log_2 \det(\mathbf{I}_M + \frac{\alpha}{\sigma^2} \mathbf{H}_1^H ((\mathbf{G}_1^H \mathbf{G}_1) \circ \Phi) \mathbf{H}_1 \mathbf{Q}) \geq t, \quad (37a)$$

$$\frac{1}{R_s} \log_2 \det(\mathbf{I}_M + \frac{\alpha}{\sigma^2} \mathbf{H}_1^H ((\mathbf{G}_2^H \mathbf{G}_2) \circ \Phi) \mathbf{H}_1 \mathbf{Q}) \geq t, \quad (37b)$$

$$\frac{\alpha L}{\gamma \sigma^2} \text{tr}(\mathbf{H}_1^H ((\mathbf{G}_2^H \mathbf{G}_2) \circ \Phi) \mathbf{H}_1 \mathbf{Q}) \geq t, \quad (37c)$$

$$t \geq 1, \quad (37d)$$

$$\Phi[k, k] = 1, \quad \forall k = 1, \dots, K. \quad (37e)$$

According to Appendix D, we know that (37a), (37b), and (37c) are all convex sets, and thus $\mathbf{P} - \mathbf{S6}$ is a convex problem, which can be optimally solved by using CVX. Note that the solution to $\mathbf{P} - \mathbf{S6}$ is one feasible solution of $\mathbf{P} - \mathbf{S5}$, and $\mathbf{P} - \mathbf{S6}$ has better convergence performance for solving $\mathbf{P} - \mathbf{S}$.

In general, the optimal solution to $\mathbf{P} - \mathbf{S6}$ may not be a rank-one matrix. Thus we need an algorithm

Algorithm 2 Solution of φ^*

Input: The solution to $\mathbf{P} - \mathbf{S6}$: Φ^*

- 1: Obtain *singular value decomposition* (SVD) for Φ^* as $\Phi^* = \mathbf{U}_1 \Sigma_1 \mathbf{U}_1^H$;
- 2: **if** $\text{Rank}(\Sigma_1) = 1$, **then**
- 3: $\varphi^* = \sqrt{\Sigma_1[1, 1]} \mathbf{U}_1^\dagger[:, 1]$;
- 4: **else**
- 5: **for** $d = 1 : D$
- 6: Generate a random vector $\varphi_d^\dagger = [\varphi_{d,1}, \dots, \varphi_{d,K}]^T = \mathbf{U}_1 \Sigma_1 \mathbf{r}_d$, where $\mathbf{r}_d \in \mathcal{CN}(0, \mathbf{I}_K)$;
- 7: Let $\varphi_{d,k} \leftarrow \frac{\varphi_{d,k}}{|\varphi_{d,k}|}$, for $k = 1, \dots, K$;
- 8: **end for**
- 9: $\varphi^* = \arg \min_{d=1:D} \text{tr}(\mathbf{Q}; \varphi_d)$;

Output: The passive beamformer φ^* .

to construct φ_k , for $k = 1, \dots, K$, from the optimal solution to the problem $\mathbf{P} - \mathbf{S6}$. In particular, after obtaining optimal Φ^* , we use Algorithm 2 to find the optimal or the approximate solution φ^* . Note that the constructed φ_d in step 6 of Algorithm 2 may not be in the set of \mathcal{A} , and thus we adjust the elements of φ_d in step 7 to make sure $\varphi_k \in \mathcal{A}$, for $k = 1, \dots, K$. In addition, after generating D random vectors $\varphi_d, d = 1, \dots, D$, we calculate $\text{tr}(\mathbf{Q})$ for a given φ_d by solving $\mathbf{P} - \mathbf{S1}$, and then we take the value of $\varphi^* = \arg \min_{d=1:D} \text{tr}(\mathbf{Q}; \varphi_d)$ as the constructed passive reflecting beamformer.

B. Overall Algorithm for Solving $\mathbf{P} - \mathbf{S}$

In this section, we present a detailed description of the proposed algorithm for solving $\mathbf{P} - \mathbf{S}$ based on the above analysis. After solving $\mathbf{P} - \mathbf{S6}$, we will obtain Φ . However, φ is needed for solving $\mathbf{P} - \mathbf{S1}$. If we execute Algorithm 2 for obtaining φ in each iteration, the convergence performance cannot be guaranteed since the derived Φ may not be a rank-one matrix. Thus, based on (31) to (33), we transform $\mathbf{P} - \mathbf{S1}$ into the following optimization problem:

$$\mathbf{P} - \mathbf{S7} : \min_{\mathbf{Q}} \quad \text{tr}(\mathbf{Q})$$

$$s.t. \quad \log_2 \det(\mathbf{I}_M + \frac{\alpha}{\sigma^2} \mathbf{H}_1^H ((\mathbf{G}_1^H \mathbf{G}_1) \circ \Phi) \mathbf{H}_1 \mathbf{Q}) \geq R_s, \quad (38a)$$

$$\log_2 \det(\mathbf{I}_M + \frac{\alpha}{\sigma^2} \mathbf{H}_1^H ((\mathbf{G}_2^H \mathbf{G}_2) \circ \Phi) \mathbf{H}_1 \mathbf{Q}) \geq R_s, \quad (38b)$$

$$\frac{\alpha L}{\sigma^2} \text{tr}(\mathbf{H}_1^H ((\mathbf{G}_2^H \mathbf{G}_2) \circ \Phi) \mathbf{H}_1 \mathbf{Q}) \geq \gamma. \quad (38c)$$

We know that solving $\mathbf{P} - \mathbf{S7}$ is equivalent to solving $\mathbf{P} - \mathbf{S1}$. Thus, we solve $\mathbf{P} - \mathbf{S7}$ and $\mathbf{P} - \mathbf{S6}$ iteratively until convergence. The details of the algorithm steps to solve $\mathbf{P} - \mathbf{S}$ are summarized in Algorithm 3.

C. Convergence and Complexity Analysis

In this section, we analyze the convergence and the computational complexity of the proposed algorithm.

Algorithm 3 Solution to $\mathbf{P} - \mathbf{S}$

- 1: Randomly generate I independent φ that satisfy $\varphi_k \in \mathcal{A}$ and calculate the minimum transmit power by solving $\mathbf{P} - \mathbf{S1}$,
 - 2: Select $\tilde{\varphi}^*$ with minimum transmit power $\text{tr}(\tilde{\mathbf{Q}}^*)$ among all I points as the initial point;
 - 3: Initialize $\mathbf{Q}^{(0)} = \tilde{\mathbf{Q}}^*$, $\Phi^{(0)} = (\tilde{\varphi}^*)^\dagger (\tilde{\varphi}^*)^T$, and $t = 0$;
 - 4: **Repeat**
 - 5: $t \leftarrow t + 1$
 - 6: Calculate $\Phi^{(t)}$ by solving $\mathbf{P} - \mathbf{S6}$ based on $\mathbf{Q}^{(t-1)}$;
 - 7: Calculate $\mathbf{Q}^{(t)}$ by solving $\mathbf{P} - \mathbf{S7}$ based on $\Phi^{(t)}$;
 - 8: **Until** the objective function of $\mathbf{P} - \mathbf{S}$ converges;
 - 9: Obtain φ^* by Algorithm 2.
 - 10: Obtain \mathbf{Q}^* by solving $\mathbf{P} - \mathbf{S1}$ based on φ^* ;
 - 11: Obtain \mathbf{W}^* based on SVD method.
-

1) *Convergence Analysis:* Since $\mathbf{P} - \mathbf{S6}$ and $\mathbf{P} - \mathbf{S7}$ are convex problems, similar to Theorem 2, we have $\text{tr}(\mathbf{Q}^{(t)}; \Phi^{(t)}) \leq \text{tr}(\mathbf{Q}^{(t-1)}; \Phi^{(t-1)})$. According to Cauchy's theorem [40], we know that when $t \rightarrow \infty$, the sequence of $(\mathbf{Q}^{(t)}, \Phi^{(t)})$ will converge to (\mathbf{Q}^*, Φ^*) , which guarantees to converge to a local (global) optimum with respect to \mathbf{Q} and Φ . The derived Φ^* may not be a rank-one matrix, which implies that the optimal objective value $\text{tr}(\mathbf{Q})$ only serves as a lower bound of $\mathbf{P} - \mathbf{S}$. Using Algorithm 2, we can construct an optimal or the approximate solution φ^* . Therefore, the proposed algorithm for solving $\mathbf{P} - \mathbf{S}$ can converge to an approximate local (global) optimum with respect to \mathbf{Q} and φ .

2) *Computational Complexity:* According to [39], the computational complexity for solving problem $\mathbf{P} - \mathbf{S7}$ is $\mathcal{O}(M^4)$ by using the path-following method to solve SDP. In addition, the computational complexity for solving the problem $\mathbf{P} - \mathbf{S6}$ is $\mathcal{O}(K^2M^2 + KM^3)$ by using the path-following method to solve SDP. Thus for each iteration, the computational complexity is $\mathcal{O}(M^4 + K^2M^2 + KM^3)$. By assuming that the number of required iterations is $\mathcal{O}(J)$, the total computational complexity of the proposed algorithm is $\mathcal{O}(J(M^4 + K^2M^2 + KM^3))$.

VI. SIMULATION RESULTS

In this section, simulation results are presented to evaluate the performance of the proposed algorithms for the joint active and passive reflecting beamforming design problem. We set $d_{h,1} = 2$ m, $d_{h,2} = 200$ m, $d_{h,3} = 1000$ m, $d_{g,1} = 999$ m, and $d_{g,2} = 199$ m. The path loss exponent γ_e is set to $\gamma_e = 2$. The path loss β at the reference distance of 1 m is set to $\beta = -30$ dB. The noise power σ^2 is set to $\sigma^2 = -90$ dBm. We also set $\kappa = 1$, $\theta^{AoA} = 0.8\pi$, $\theta^{AoD} = 0.6\pi$, $\frac{d_a}{\lambda} = \frac{1}{2}$, $D = 20$, $I = 20$, $L = 50$, and $\alpha = 1$. In addition, for comparison, we consider the benchmark algorithms: random beamforming policy, and the case without LISA assistance. For the random beamforming policy, we randomly choose a complex value in the feasible set \mathcal{A} for each element at LISA, and then we solve $\mathbf{P2} - \mathbf{a}$ or $\mathbf{P} - \mathbf{S1}$ based on the random φ . For the case

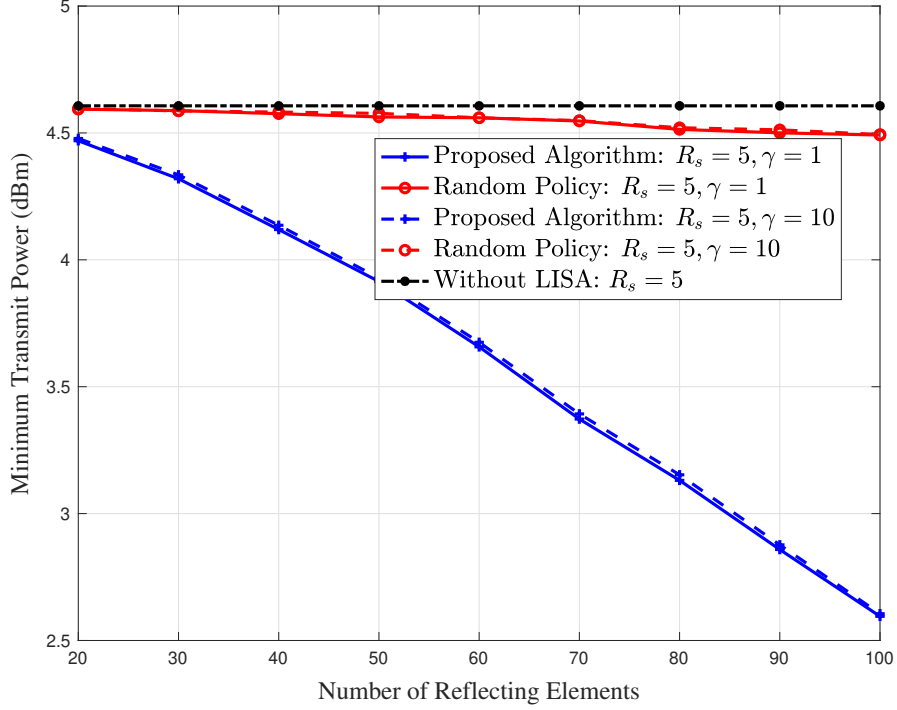


Fig. 3: The minimum transmit power required at BS versus the number K of reflecting elements at LISA for the general case.

without LISA assistance, we solve the following optimization problem and set the optimal beamformer at BS.

$$\begin{aligned}
 \mathbf{P} - \mathbf{W} : \quad & \min_{\mathbf{Q}} \text{tr}(\mathbf{Q}) \\
 & s.t. \quad \log_2 \det(\mathbf{I}_{N_1} + \frac{1}{\sigma^2} \mathbf{H}_2 \mathbf{Q} \mathbf{H}_2^H) \geq R_s.
 \end{aligned} \tag{39a}$$

A. Performance of the Proposed Algorithm

Fig. 3 illustrates the minimum transmit power required at BS versus the number of reflecting elements at LISA under different policies and different γ . The number of transmit antennas is set to $M = 3$ and the number of the receive antennas is set to $N_1 = N_2 = 3$. From this figure, it can be seen that the minimum transmit power decreases as the increase of the number of the reflecting elements, which means the more reflecting elements, the better performance the LISA-assisted SR system achieves. In addition, we can find that the minimum transmit power increases with the required IoT transmission SNR γ . This observation indicates that when the required IoT transmission SNR increases, the minimum transmit power increases to support the IoT transmission. However, from Fig. 3, when γ increases, the increase of the minimum transmit power is not obvious since the LISA-assisted SR system mainly meets the primary rate constraint in that case. We see that the performance of the LISA-assisted SR system is better than that without LISA. That is to

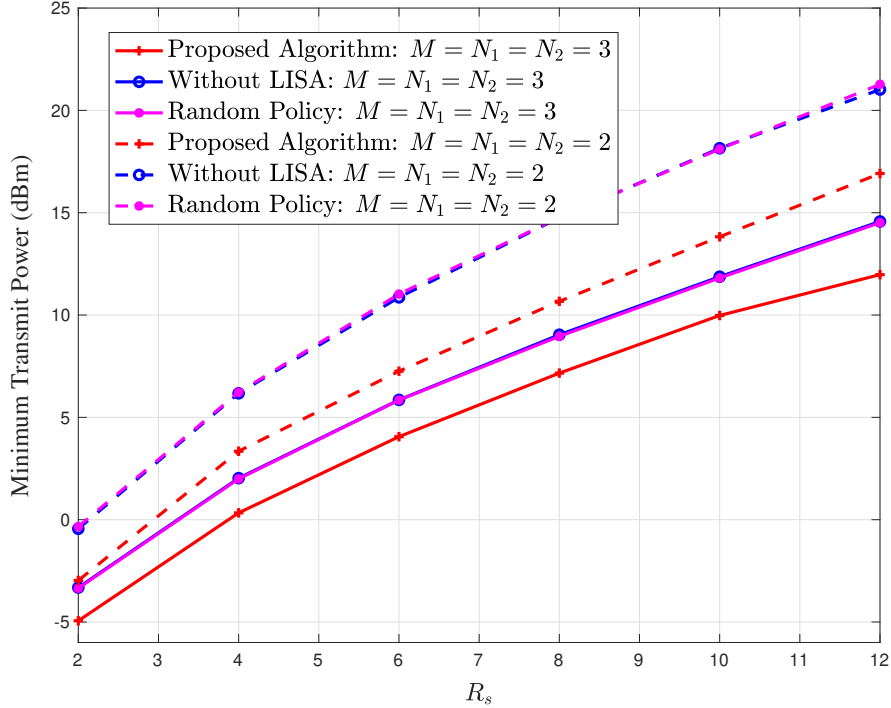


Fig. 4: The minimum transmit power versus the required transmission rate R_s for the general case.

say, with a large number of reflecting elements, the use of LISA can not only enhance the performance of the primary system but also support the IoT transmission without increasing power consumption. Furthermore, it can be seen that the proposed algorithm performs better than the random beamforming policy, which validates the effectiveness of the proposed algorithms.

Fig. 4 plots the minimum transmit power versus the required primary transmission rate R_s under different beamforming algorithms with $K = 100$. From this figure, we can find that the minimum transmit power increases with the required transmission rate R_s . Also, the performance of the proposed algorithm is better than the random policy and the case without LISA. In addition, it can be seen that the performance gap between the proposed algorithm and the case without LISA increases with the increase of R_s . The main reason is that when R_s is small, the LISA-assisted SR system needs more power to support the IoT transmission, while when R_s is large, the LISA-assisted SR system focuses on the primary transmission and the IoT transmission can be an additional benefit. Furthermore, when M, N_1, N_2 increase, the minimum transmit power increases, since the increase of antennas can enhance the system performance.

Fig. 5 shows the minimum transmit power versus the number of reflecting elements at LISA under different policies with different γ for the special case that the direct link signals are blocked. We set $M = N_1 = N_2 = 3$. Note that the lower bound denotes the minimum transmit power obtained based on Φ . The gap between

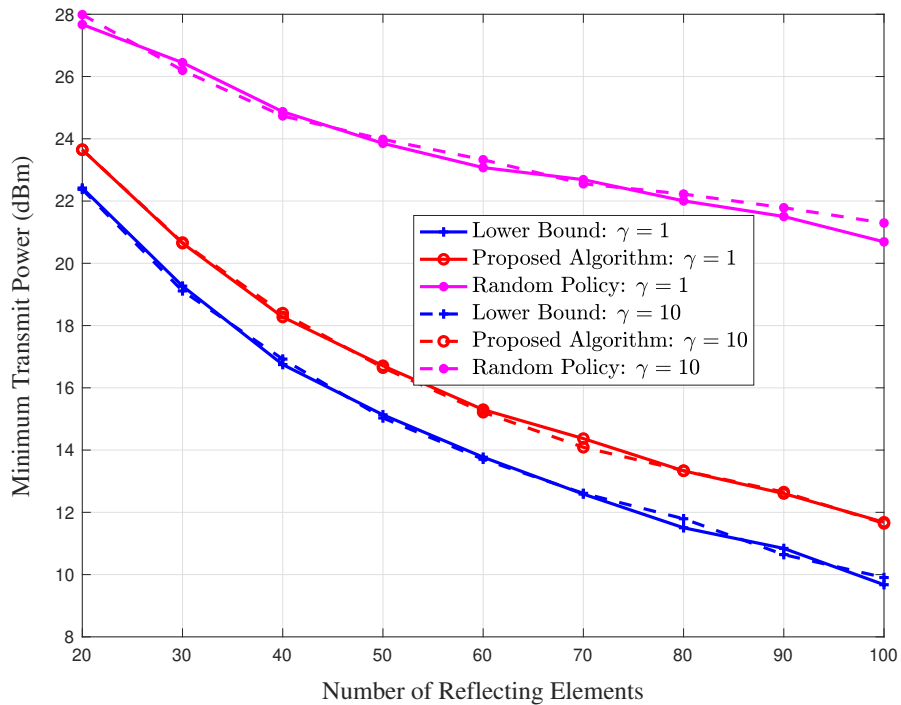


Fig. 5: The minimum transmit power versus the number K of reflecting elements at LISA for the special case.

proposed algorithm and the lower bound comes from the approximate of SDR [41]. From this figure, it can be seen that the proposed algorithm performs better than the random beamforming policy, which validates the effectiveness of the proposed algorithms. The minimum transmit power of the proposed algorithm with $K = 25$ is the same as that of the random policy with $K = 80$. In addition, we find that the change of γ from $\gamma = 1$ to $\gamma = 10$ does not affect the minimum transmit power, since the LISA-assisted SR system focuses on enhancing the performance of the primary transmission. By comparing Fig. 5 and Fig. 3, we can find that the passive reflecting beamforming gain of the proposed algorithm without direct links signal is larger than that of the proposed algorithm with the direct link signal. The main reason is that due to the double fading, the strength of the direct links signal is much stronger than that of the backscatter link signal, and thus the effect of the reflecting elements adjustment is not obvious when there exist direct link signals with small number of reflecting elements.

Fig. 6 illustrates the minimum transmit power versus the required transmission rate R_s under different beamforming algorithms for the case that the direct link signals are blocked with $K = 100$. It is obvious that the proposed algorithm performs better than the random policy. When the transmit power is 15 dBm with $M = N_1 = N_2 = 3$, the achievable transmission rate at BS of the proposed algorithm is larger than 7.5 bps/Hz, while the achievable transmission rate at BS of the random policy is 2.5 bps/Hz only. In addition, the

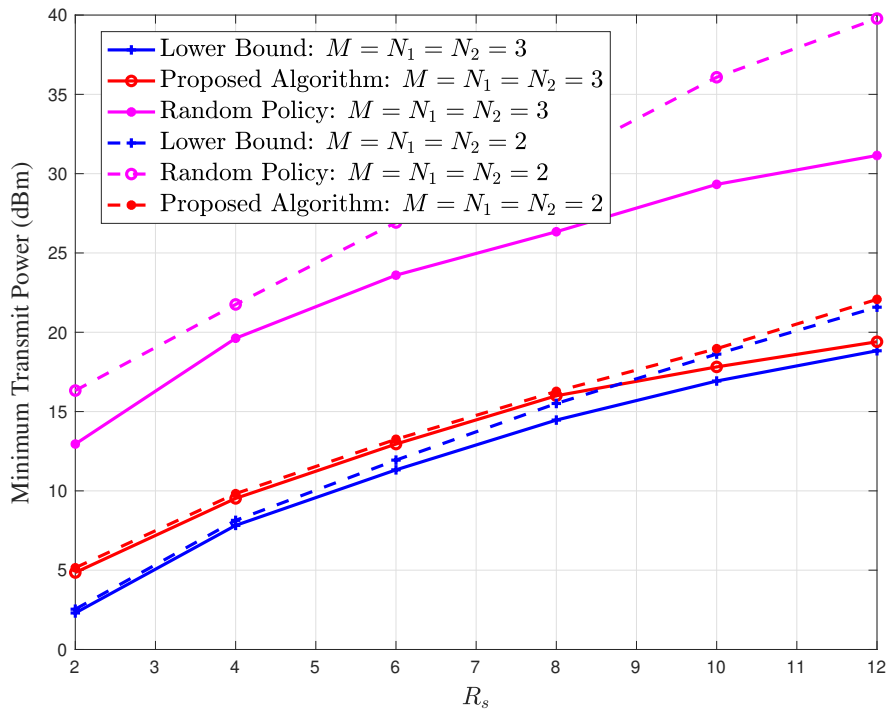


Fig. 6: The minimum transmit power versus the required transmission rate R_s for the special case.

increase of the number of antennas will enhance the performance of the proposed LISA-assisted SR system. Furthermore, the gap between the lower bound and the proposed algorithm decreases with the increase of R_s and the decrease of the number of active antennas.

B. Convergence Performance of the Proposed Algorithm

Fig. 7 plots the minimum transmit power versus the number of the iterations under different transmission rate and SNR requirements with $K = 100$ in one channel realization. We set $M = N_1 = N_2 = 3$. From this figure, we can find that the minimum transmit power increases as the increase of R_s or γ . In addition, it can be seen that the minimum transmit power converges with 4 – 5 iterations.

Fig. 8 illustrates the slack variable t versus K multiplying the number of the iterations under different transmission rate and SNR requirements with $K = 100$ in one channel realization. We set $M = N_1 = N_2 = 3$. From this figure, we can see that in each iteration, the slack variable t increases with the gradual update of the reflecting coefficient φ_k , which validates the analysis in Section IV-D1. After one iteration, the slack variable t increases from $t = 1$, since the active beamforming matrix \mathbf{W} is optimized to minimize the transmit power, which guarantees the convergence of the proposed algorithm. In addition, the slack variable t approaches to 1 with 4 – 5 iterations, which has the same conclusion as Fig. 7.

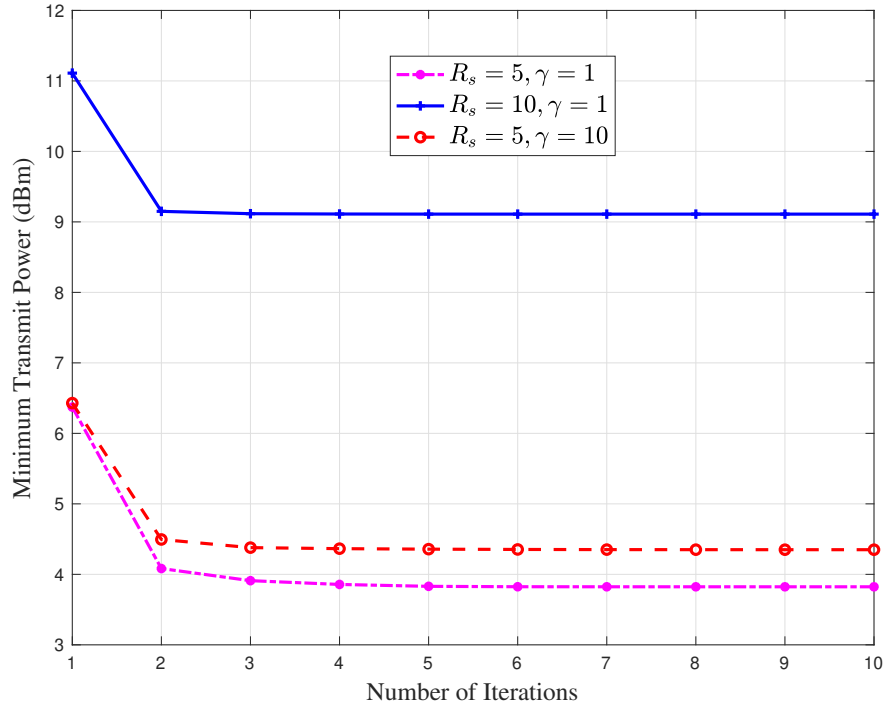


Fig. 7: Minimum transmit power versus the number of the iterations for the general case.

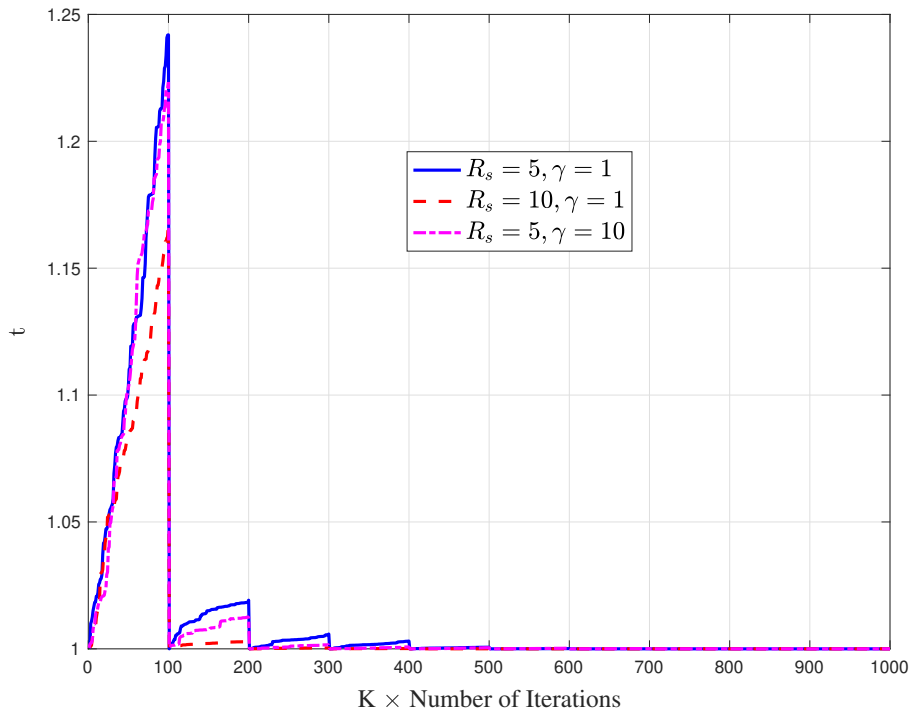


Fig. 8: Slack variable t versus K multiplying the number of the iterations for the general case.

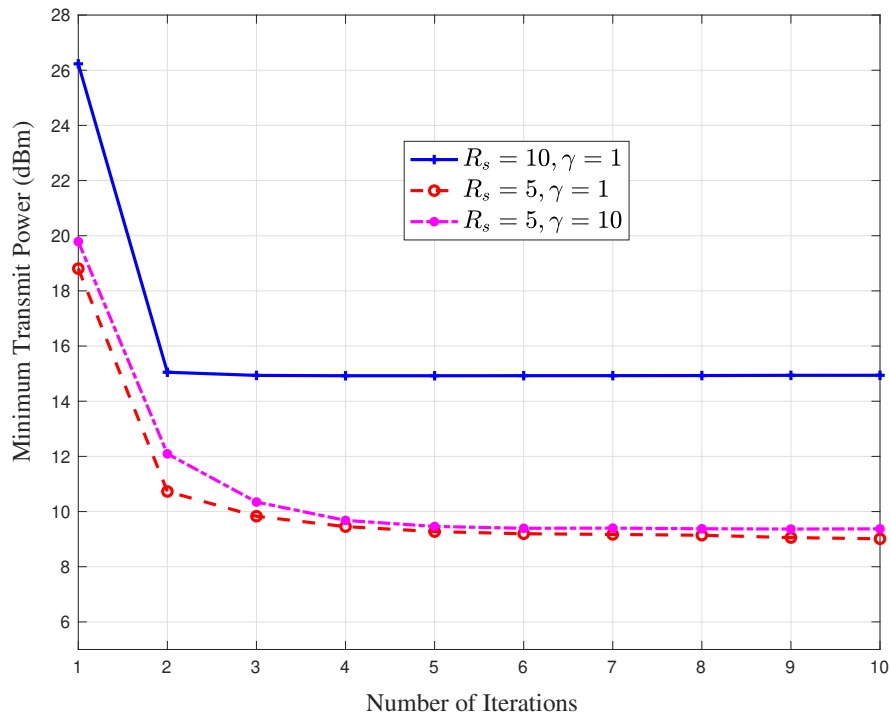


Fig. 9: Convergence performance for the special case.

Fig. 9 shows the minimum transmit power versus the number of the iterations under different transmission rate and SNR requirements with $K = 100$ in one channel realization for the special case that the direct links signals are blocked. We set $M = N_1 = N_2 = 3$. From this figure, one can see that the higher R_s or γ is, the higher the minimum transmit power is. Also, it can be seen that the minimum transmit power converges with 3 – 4 iterations, and the minimum transmit power decreases obviously compared with the initial point.

VII. CONCLUSIONS

This paper has proposed a LISA-assisted SR system and studied the joint design problem for active transmit beamformer at BS and passive reflecting beamformer at LISA which minimizes the BS total transmit power subject to the rate constraint for the primary transmission and the SNR constraint for the IoT communication. For the general case, by leveraging the AO technique, the formulated problem is decoupled into $K + 1$ subproblems, which are solved based on KKT conditions and projection method. We also consider the special case that the direct links from BS to PR and IR are blocked, in which the formulated optimization problem is decoupled into two subproblems, one of which is solved by using SDR technique. The convergence performance and the computational complexity of the proposed algorithms are analyzed for both cases. Finally, simulation results have demonstrated the effectiveness of the proposed algorithms and validated the advantages of the LISA-assisted SR system.

APPENDIX A

According to [9], when IR jointly decodes $\mathbf{s}(l)$ and c , the backscatter link can be treated as a multi-path component from BS to IR, and thus the signal-plus-noise covariance matrix is given by

$$\mathbf{\Gamma}_{b,s} = (\mathbf{H}_2 + \sqrt{\alpha}c\mathbf{G}_2\mathbf{\Psi}\mathbf{H}_1)\mathbf{W}\mathbf{W}^H(\mathbf{H}_2 + \sqrt{\alpha}c\mathbf{G}_2\mathbf{\Psi}\mathbf{H}_1)^H. \quad (40)$$

Since the symbol period of c covers L symbol periods of \mathbf{s} , by using the *maximal ratio combining* (MRC), the SNR for decoding c is given by

$$\begin{aligned} \gamma_{b,c} &= \frac{\alpha}{\sigma^2} \sum_{l=1}^L \|\sqrt{\alpha}c\mathbf{G}_2\mathbf{\Psi}\mathbf{H}_1\mathbf{W}\mathbf{s}(l)\|^2 = \frac{\alpha}{\sigma^2} \sum_{l=1}^L \text{tr}(\mathbf{G}_2\mathbf{\Psi}\mathbf{H}_1\mathbf{W}\mathbf{s}(l)\mathbf{s}^H(l)\mathbf{W}^H\mathbf{H}_1^H\mathbf{\Psi}^H\mathbf{G}_2^H) \\ &\stackrel{(a)}{=} \frac{\alpha L}{\sigma^2} \text{tr}(\mathbf{G}_2\mathbf{\Psi}\mathbf{H}_1\mathbf{W}\mathbb{E}[\mathbf{s}(l)\mathbf{s}^H(l)]\mathbf{W}^H\mathbf{H}_1^H\mathbf{\Psi}^H\mathbf{G}_2^H) = \frac{\alpha L}{\sigma^2} \text{tr}(\mathbf{G}_2\mathbf{\Psi}\mathbf{H}_1\mathbf{W}\mathbf{W}^H\mathbf{H}_1^H\mathbf{\Psi}^H\mathbf{G}_2^H), \end{aligned} \quad (41)$$

when $L \gg 1$, (a) holds since the arithmetic mean approaches the statistical expectation.

APPENDIX B

By substituting (14) into (13), the received signal at IR is $y_b = \sqrt{\alpha}sc \sum_{k=0}^{K-1} e^{jk\frac{2\pi d_a}{\lambda}(\sin\psi + \sin\theta_1 - \sin\theta_2)}$. The strength of the backscatter link signal is $\alpha|s|^2|c|^2|\sum_{k=0}^{K-1} e^{jk\frac{2\pi d_a}{\lambda}(\sin\psi + \sin\theta_1 - \sin\theta_2)}|^2$, which is maximized when $\sin\psi + \sin\theta_1 - \sin\theta_2 = \frac{\ell\lambda}{d_a}$ for arbitrary integer ℓ .

APPENDIX C

First, we expand f_3 to

$$\begin{aligned} f_3(\varphi_k) &= \log_2 \det(\mathbf{I}_{N_1} + \frac{1}{\sigma^2}(\mathbf{H}_3 + \mathbf{F}_1)\mathbf{Q}(\mathbf{H}_3 + \mathbf{F}_1)^H) \\ &= \log_2 \det(\mathbf{I}_{N_1} + \frac{1}{\sigma^2}(\mathbf{H}_3 + \sqrt{\alpha} \sum_{k=1}^K \varphi_k \mathbf{g}_{1,k} \mathbf{h}_{1,k}^H)\mathbf{Q}(\mathbf{H}_3 + \sqrt{\alpha} \sum_{k=1}^K \varphi_k \mathbf{g}_{1,k} \mathbf{h}_{1,k}^H)^H) \\ &= \log_2 \det(\mathbf{I}_{N_1} + \frac{1}{\sigma^2}\mathbf{H}_3\mathbf{Q}\mathbf{H}_3^H + \frac{\sqrt{\alpha}}{\sigma^2} \sum_{k=1}^K \varphi_k \mathbf{g}_{1,k} \mathbf{h}_{1,k}^H \mathbf{Q}\mathbf{H}_3^H + \frac{\sqrt{\alpha}}{\sigma^2}\mathbf{H}_3\mathbf{Q} \sum_{k=1}^K \varphi_k^\dagger \mathbf{h}_{1,k} \mathbf{g}_{1,k}^H \\ &\quad + \frac{\alpha}{\sigma^2} \sum_{k_1=1}^K \sum_{k_2=1}^K \varphi_{k_1} \varphi_{k_2}^\dagger \mathbf{g}_{1,k_1} \mathbf{h}_{1,k_1}^H \mathbf{Q}\mathbf{h}_{1,k_2} \mathbf{g}_{1,k_2}^H) \\ &\stackrel{(a)}{=} \log_2 \det(\mathbf{A}_{1,k} + \varphi_k \mathbf{B}_{1,k} + \varphi_k^\dagger \mathbf{B}_{1,k}^H), \end{aligned} \quad (42)$$

where (a) holds due to $|\varphi_k|^2 = 1$. Next, we will further simplify (42). It is obvious that $\mathbf{A}_{1,k}$ is a full rank matrix. Thus matrix $\mathbf{A}_{1,k}$ is invertible, and we have $\log_2 \det(\mathbf{A}_{1,k} + \varphi_k \mathbf{B}_{1,k} + \varphi_k^\dagger \mathbf{B}_{1,k}^H) = \log_2 \det(\mathbf{A}_{1,k}) + g_1$, where $g_1 = \log_2 \det(\mathbf{I}_{N_1} + \varphi_k \mathbf{A}_{1,k}^{-1} \mathbf{B}_{1,k} + \varphi_k^\dagger \mathbf{A}_{1,k}^{-1} \mathbf{B}_{1,k}^H)$. Since the rank of $\mathbf{B}_{1,k}$ is one, we have $\text{rank}(\mathbf{A}_{1,k}^{-1} \mathbf{B}_{1,k}) \leq \text{rank}(\mathbf{B}_{1,k}) \leq 1$. If $\text{rank}(\mathbf{A}_{1,k}^{-1} \mathbf{B}_{1,k}) = 0$, we have $\mathbf{A}_{1,k}^{-1} \mathbf{B}_{1,k} = \mathbf{0}$. In that case, we have $\mathbf{A}_{1,k}^{-1} \mathbf{B}_{1,k}^H = \mathbf{A}_{1,k}^{-1} \mathbf{B}_{1,k}^H (\mathbf{A}_{1,k}^H)^{-1} \mathbf{A}_{1,k}^H = \mathbf{A}_{1,k}^{-1} (\mathbf{A}_{1,k}^{-1} \mathbf{B}_{1,k})^H \mathbf{A}_{1,k}^H = \mathbf{0}$, and thus $\log_2 \det(\mathbf{A}_{1,k} + \varphi_k \mathbf{B}_{1,k} + \varphi_k^\dagger \mathbf{B}_{1,k}^H) = \log_2 \det(\mathbf{A}_{1,k})$, which is independent of the reflecting coefficient φ_k . When $\text{rank}(\mathbf{A}_{1,k}^{-1} \mathbf{B}_{1,k}) = 1$, if there is no non-zero eigenvalue for matrix $\mathbf{A}_{1,k}^{-1} \mathbf{B}_{1,k}$, it becomes a nilpotent matrix, which satisfies $\text{tr}(\mathbf{A}_{1,k}^{-1} \mathbf{B}_{1,k}) = 0$

[27], [42]. In that case, we have $\log_2 \det(\mathbf{A}_{1,k} + \varphi_k \mathbf{B}_{1,k} + \varphi_k^\dagger \mathbf{B}_{1,k}^H) = \log_2 \det(\mathbf{A}_{1,k} - \mathbf{B}_{1,k}^H \mathbf{A}_{1,k}^{-1} \mathbf{B}_{1,k})$, which is also independent of the reflecting coefficient φ_k . Next, we consider the case with non-zero eigenvalue for matrix $\mathbf{A}_{1,k}^{-1} \mathbf{B}_{1,k}$ and $\text{rank}(\mathbf{A}_{1,k}^{-1} \mathbf{B}_{1,k}) = 1$. In that case, the eigendecomposition of matrix $\mathbf{A}_{1,k}^{-1} \mathbf{B}_{1,k}$ exists, which can be expressed as $\mathbf{A}_{1,k}^{-1} \mathbf{B}_{1,k} = \mathbf{U}_{1,k} \boldsymbol{\Sigma}_{1,k} \mathbf{U}_{1,k}^{-1}$, where $\boldsymbol{\Sigma}_{1,k} = \text{diag}\{\lambda_{1,k}, 0, \dots, 0\}$, $\lambda_{1,k}$ is the non-zero eigenvalue of matrix $\mathbf{A}_{1,k}^{-1} \mathbf{B}_{1,k}$. Therefore, g_1 can be simplified as

$$\begin{aligned} g_1 &= \log_2 \det(\mathbf{I}_{N_1} + \varphi_k \mathbf{U}_{1,k} \boldsymbol{\Sigma}_{1,k} \mathbf{U}_{1,k}^{-1} + \varphi_k^\dagger \mathbf{A}_{1,k}^{-1} (\mathbf{U}_{1,k} \boldsymbol{\Sigma}_{1,k} \mathbf{U}_{1,k}^{-1})^H \mathbf{A}_{1,k}^H) \\ &\stackrel{(a)}{=} \log_2 \det(\mathbf{I}_{N_1} + \varphi_k \boldsymbol{\Sigma}_{1,k} + \varphi_k^\dagger \mathbf{U}_{1,k}^{-1} \mathbf{A}_{1,k}^{-1} (\mathbf{U}_{1,k}^{-1})^H \boldsymbol{\Sigma}_{1,k}^H \mathbf{U}_{1,k}^H \mathbf{A}_{1,k}^H \mathbf{U}_{1,k}) \\ &\stackrel{(b)}{=} \log_2 \det(\mathbf{I}_{N_1} + \varphi_k \boldsymbol{\Sigma}_{1,k} + \varphi_k^\dagger \mathbf{V}_{1,k}^{-1} \boldsymbol{\Sigma}_{1,k}^H \mathbf{V}_{1,k}), \end{aligned} \quad (43)$$

where (a) holds by multiplying $\det(\mathbf{U}_{1,k}^{-1}) \det(\mathbf{U}_{1,k})$, (b) holds due to $\mathbf{A}_{1,k}^H = \mathbf{A}_{1,k}$, and $\mathbf{V}_{1,k} = \mathbf{U}_{1,k}^H \mathbf{A}_{1,k} \mathbf{U}_{1,k}$. Since $\boldsymbol{\Sigma}_{1,k} = \text{diag}\{\lambda_{1,k}, 0, \dots, 0\}$, we have $\mathbf{V}_{1,k}^{-1} \boldsymbol{\Sigma}_{1,k}^H \mathbf{V}_{1,k} = \lambda_{1,k}^\dagger \mathbf{v}_{1,k} \tilde{\mathbf{v}}_{1,k}^T$, where $\mathbf{v}_{1,k}$ is the first column of $\mathbf{V}_{1,k}^{-1}$, $\tilde{\mathbf{v}}_{1,k}^T$ is the first row of $\mathbf{V}_{1,k}$. Thus, g_1 can be further simplified as

$$\begin{aligned} g_1 &= \log_2 \det(\mathbf{I}_{N_1} + \varphi_k \boldsymbol{\Sigma}_{1,k} + \varphi_k^\dagger \lambda_{1,k}^\dagger \mathbf{v}_{1,k} \tilde{\mathbf{v}}_{1,k}^T) \\ &\stackrel{(a)}{=} \log_2(1 + \varphi_k^\dagger \lambda_{1,k}^\dagger \tilde{\mathbf{v}}_{1,k}^T (\mathbf{I}_{N_1} + \varphi_k \boldsymbol{\Sigma}_{1,k})^{-1} \mathbf{v}_{1,k}) + \log_2 \det(\mathbf{I}_{N_1} + \varphi_k \boldsymbol{\Sigma}_{1,k}) \\ &= \log_2 \left(1 + \varphi_k^\dagger \lambda_{1,k}^\dagger \tilde{\mathbf{v}}_{1,k}^T \left(\mathbf{I}_{N_1} - \text{diag} \left\{ \frac{\varphi_k \lambda_{1,k}}{1 + \varphi_k \lambda_{1,k}}, 0, \dots, 0 \right\} \right) \mathbf{v}_{1,k} \right) + \log_2(1 + \varphi_k \lambda_{1,k}) \\ &\stackrel{(b)}{=} \log_2 \left(\left(1 + \varphi_k^\dagger \lambda_{1,k}^\dagger - \frac{|\lambda_{1,k}|^2 \tilde{v}_{1,k} v_{1,k}}{1 + \varphi_k \lambda_{1,k}} \right) (1 + \varphi_k \lambda_{1,k}) \right) \\ &= \log_2 \left(\left(1 + \varphi_k^\dagger \lambda_{1,k}^\dagger \right) (1 + \varphi_k \lambda_{1,k}) - |\lambda_{1,k}|^2 \tilde{v}_{1,k} v_{1,k} \right) \\ &= \log_2 (1 + |\lambda_{1,k}|^2 (1 - \tilde{v}_{1,k} v_{1,k}) + 2\text{Re}(\varphi_k \lambda_{1,k})), \end{aligned} \quad (44)$$

where (a) holds due to the fact that $\det(\mathbf{X} + \mathbf{A}\mathbf{B}) = \det(\mathbf{X}) \det(\mathbf{I} + \mathbf{B}\mathbf{X}^{-1}\mathbf{A})$, (b) holds due to $\tilde{\mathbf{v}}_{1,k}^T \mathbf{v}_{1,k} = 1$ according to $\mathbf{V}_{1,k} \mathbf{V}_{1,k}^{-1} = \mathbf{I}$, $\tilde{v}_{1,k}$ is the first element of $\tilde{\mathbf{v}}_{1,k}^T$, and $v_{1,k}$ is the first element of $\mathbf{v}_{1,k}$. Since $\mathbf{V}_{1,k}$ and $\mathbf{V}_{1,k}^{-1}$ are Hermitian matrices, we have both $v_{1,k}$ and $\tilde{v}_{1,k}$ are real values. Therefore, we have

$$f_3(\varphi_k) = \begin{cases} \log_2 \det(\mathbf{A}_{1,k}), & \text{if } \text{rank}(\mathbf{A}_{1,k}^{-1} \mathbf{B}_{1,k}) = 0, \\ \log_2 \det(\mathbf{A}_{1,k} - \mathbf{B}_{1,k}^H \mathbf{A}_{1,k}^{-1} \mathbf{B}_{1,k}), & \text{if } \text{rank}(\mathbf{A}_{1,k}^{-1} \mathbf{B}_{1,k}) = 1, \text{tr}(\mathbf{A}_{1,k}^{-1} \mathbf{B}_{1,k}) = 0, \\ \log_2 (1 + |\lambda_{1,k}|^2 (1 - \tilde{v}_{1,k} v_{1,k}) + 2\text{Re}(\varphi_k \lambda_{1,k})) + \log_2 \det(\mathbf{A}_{1,k}), & \text{otherwise} \end{cases}$$

In the same way, we can simplify f_4 , f_5 , and f_6 . For f_7 , we have the following equations:

$$\begin{aligned} f_7(\varphi_k) &\triangleq \frac{L}{\sigma^2} \text{tr}(\mathbf{F}_2 \mathbf{Q} \mathbf{F}_2^H) = \frac{\alpha L}{\sigma^2} \text{tr} \left(\left(\sum_{k=1}^K \varphi_k \mathbf{g}_{2,k} \mathbf{h}_{1,k}^H \right) \mathbf{Q} \left(\sum_{k=1}^K \varphi_k^\dagger \mathbf{h}_{1,k} \mathbf{g}_{2,k}^H \right) \right) \\ &\stackrel{(a)}{=} \frac{\alpha L}{\sigma^2} \text{tr} \left(\sum_{k_1=1}^K \sum_{k_2=1}^K \varphi_{k_1} \varphi_{k_2}^\dagger \mathbf{g}_{2,k_2}^H \mathbf{g}_{2,k_1} \mathbf{h}_{1,k_1}^H \mathbf{Q} \mathbf{h}_{1,k_2} \right) = \frac{\alpha L}{\sigma^2} (A_{5,k} + 2\text{Re}(\varphi_k B_{5,k})) \end{aligned}$$

where (a) is based on the property of trace. i.e., $\text{tr}(\mathbf{X}_1\mathbf{X}_2) = \text{tr}(\mathbf{X}_2\mathbf{X}_1)$.

Therefore, Theorem 1 is proved.

APPENDIX D

Let $f(\mathbf{X}) = \log_2 \det(\mathbf{I}_n + \mathbf{B}^H(\mathbf{A} \circ \mathbf{X})\mathbf{B})$, where \mathbf{A} and \mathbf{X} are Hermitian matrices, and we verify the concavity of $f(\mathbf{X})$. First, Let us consider an arbitrary line represented by $\mathbf{X} = \mathbf{Z} + t\mathbf{V}$, where \mathbf{Z} and \mathbf{V} are Hermitian matrices. Then, we need to verify the concavity of $f(\mathbf{X})$ by analyzing $g(t) \triangleq f(\mathbf{Z} + t\mathbf{V})$, where t satisfies the condition that $\mathbf{I}_n + \mathbf{B}^H(\mathbf{A} \circ (\mathbf{Z} + t\mathbf{V}))\mathbf{B}$ is a positive definite matrix due to the constraint of the domain of function f [38]. Without loss of generality, we assume that $t = 0$ is inside this interval, i.e., $\mathbf{I}_n + \mathbf{B}^H(\mathbf{A} \circ \mathbf{Z})\mathbf{B}$ is a positive definite matrix. Then, we have

$$g(t) = \log_2 \det(\mathbf{I}_n + \mathbf{B}^H(\mathbf{A} \circ (\mathbf{Z} + t\mathbf{V}))\mathbf{B}) = \log_2 \det(\mathbf{I}_n + \mathbf{B}^H(\mathbf{A} \circ \mathbf{Z})\mathbf{B} + t\mathbf{B}^H(\mathbf{A} \circ \mathbf{V})\mathbf{B}).$$

By letting $\mathbf{K} \triangleq \mathbf{I}_n + \mathbf{B}^H(\mathbf{A} \circ \mathbf{Z})\mathbf{B}$, we have

$$\begin{aligned} g(t) &= \log_2 \det(\mathbf{K} + t\mathbf{B}^H(\mathbf{A} \circ \mathbf{V})\mathbf{B}) = \log_2 \det(\mathbf{K}^{\frac{1}{2}}(\mathbf{I}_n + t\mathbf{K}^{-\frac{1}{2}}\mathbf{B}^H(\mathbf{A} \circ \mathbf{V})\mathbf{B}\mathbf{K}^{-\frac{1}{2}})\mathbf{K}^{\frac{1}{2}}) \\ &= \log_2 \det(\mathbf{K}) + \log_2 \det(\mathbf{I}_n + t\mathbf{K}^{-\frac{1}{2}}\mathbf{B}^H(\mathbf{A} \circ \mathbf{V})\mathbf{B}\mathbf{K}^{-\frac{1}{2}}). \end{aligned}$$

It is obvious that \mathbf{K} and $\mathbf{B}^H(\mathbf{A} \circ \mathbf{V})\mathbf{B}$ are Hermitian matrices, and thus $\mathbf{K}^{-\frac{1}{2}}\mathbf{B}^H(\mathbf{A} \circ \mathbf{V})\mathbf{B}\mathbf{K}^{-\frac{1}{2}}$ is a Hermitian matrix. According to eigendecomposition, we have $\mathbf{K}^{-\frac{1}{2}}\mathbf{B}^H(\mathbf{A} \circ \mathbf{V})\mathbf{B}\mathbf{K}^{-\frac{1}{2}} = \mathbf{U}\mathbf{\Lambda}\mathbf{U}^H$, where $\mathbf{U}\mathbf{U}^H = \mathbf{I}_n$ and $\mathbf{\Lambda}$ is the diagonal matrix generated by the eigenvalues of $\mathbf{K}^{-\frac{1}{2}}\mathbf{B}^H(\mathbf{A} \circ \mathbf{V})\mathbf{B}\mathbf{K}^{-\frac{1}{2}}$, $\beta_i, i = 1, \dots, n$.

Thus, we have

$$\begin{aligned} g(t) &= \log_2 \det(\mathbf{K}) + \log_2 \det(\mathbf{I}_n + t\mathbf{U}\mathbf{\Lambda}\mathbf{U}^H) = \log_2 \det(\mathbf{K}) + \log_2 \det(\mathbf{U}\mathbf{U}^H + t\mathbf{U}\mathbf{\Lambda}\mathbf{U}^H) \\ &= \log_2 \det(\mathbf{K}) + \log_2 \det(\mathbf{U}(\mathbf{I}_n + t\mathbf{\Lambda})\mathbf{U}^H) \stackrel{(a)}{=} \log_2 \det(\mathbf{K}) + \log_2 \det(\mathbf{I}_n + t\mathbf{\Lambda}) \\ &\stackrel{(b)}{=} \log_2 \det(\mathbf{K}) + \log_2 \left(\prod_{i=1}^n (1 + t\beta_i) \right) = \log_2 \det(\mathbf{K}) + \sum_{i=1}^n \log_2(1 + t\beta_i). \end{aligned}$$

where (a) holds due to $\det(\mathbf{U}\mathbf{U}^H) = 1$, and (b) holds based on the definition of determinant. It is easy to seen that $g(t) = \log_2 \det(\mathbf{K}) + \sum_{i=1}^n \log_2(1 + t\beta_i)$ is a concave function. Therefore, $f(\mathbf{X})$ is a concave function.

Based on the above analysis, we have the following results. Since $\mathbf{Q} = \mathbf{W}\mathbf{W}^H$, we have $\log_2 \det(\mathbf{I}_M + \frac{\alpha}{\sigma^2} \mathbf{H}_1^H ((\mathbf{G}_1^H \mathbf{G}_1) \circ \mathbf{\Phi}) \mathbf{H}_1 \mathbf{Q}) = \log_2 \det(\mathbf{I}_M + \frac{\alpha}{\sigma^2} \mathbf{W}^H \mathbf{H}_1^H ((\mathbf{G}_1^H \mathbf{G}_1) \circ \mathbf{\Phi}) \mathbf{H}_1 \mathbf{W})$, which is a concave function with respect to $\mathbf{\Phi}$. Similarly, $\log_2 \det(\mathbf{I}_M + \frac{\alpha}{\sigma^2} \mathbf{H}_1^H ((\mathbf{G}_2^H \mathbf{G}_2) \circ \mathbf{\Phi}) \mathbf{H}_1 \mathbf{Q})$ is a concave function with respect to $\mathbf{\Phi}$. It is obvious that $\text{tr}(\mathbf{H}_1^H ((\mathbf{G}_2^H \mathbf{G}_2) \circ \mathbf{\Phi}) \mathbf{H}_1 \mathbf{Q})$ is a linear function with respect to $\mathbf{\Phi}$. Therefore, the constraints (37a), (37b), and (37c) are all convex sets.

REFERENCES

- [1] Q. Zhang, Y.-C. Liang, and H. V. Poor, "Symbiotic radio: A new application of largeintelligent surface/antennas (LISA)," *IEEE Wireless Commun. Netw. Conf. (WCNC)*, accepted, 2020.
- [2] M. Latva-aho and K. Leppanen, "Key drivers and research challenges for 6G ubiquitous wireless intelligence," *University of Oulu, White Paper*, 2019. Available: <http://urn.fi/urn:isbn:9789526223544>.
- [3] L. Zhang, Y.-C. Liang, and D. Niyato, "6G visions: Mobile ultra-broadband, super internet-of-things, and artificial intelligence," *China Commun.*, vol. 16, no. 8, pp. 1–14, 2019.
- [4] L. Zhang, Y.-C. Liang, and M. Xiao, "Spectrum sharing for internet of things: A survey," *IEEE Wireless Commun.*, vol. 26, no. 3, pp. 132–139, 2018.
- [5] X. Kang, Y.-C. Liang, and J. Yang, "Riding on the primary: A new spectrum sharing paradigm for wireless-powered IoT devices," *IEEE Trans. Wireless Commun.*, vol. 17, no. 9, pp. 6335–6347, Sep. 2018.
- [6] V. Liu, A. Parks, V. Talla, S. Gollakota, D. Wetherall, and J. R. Smith, "Ambient backscatter: Wireless communication out of thin air," *Proc. ACM SIGCOMM*, vol. 43, no. 4, pp. 39–50, Oct. 2013.
- [7] G. Yang, Y.-C. Liang, R. Zhang, and Y. Pei, "Modulation in the air: Backscatter communication over ambient OFDM carrier," *IEEE Trans. Commun.*, vol. 66, no. 3, pp. 1219–1233, Mar. 2018.
- [8] J. Qian, F. Gao, G. Wang, S. Jin, and H. Zhu, "Noncoherent detections for ambient backscatter system," *IEEE Trans. Wireless Commun.*, vol. 16, no. 3, pp. 1412–1422, Mar. 2017.
- [9] G. Yang, Q. Zhang, and Y.-C. Liang, "Cooperative ambient backscatter communications for green Internet-of-Things," *IEEE Internet Things J.*, vol. 5, no. 2, pp. 1116–1130, Apr. 2018.
- [10] W. Liu, Y.-C. Liang, Y. Li, and B. Vucetic, "Backscatter multiplicative multiple-access systems: Fundamental limits and practical design," *IEEE Trans. Wireless Commun.*, vol. 17, no. 9, pp. 5713–5728, 2018.
- [11] R. Long, Y.-C. Liang, H. Guo, G. Yang, and R. Zhang, "Symbiotic radio: A new communication paradigm for passive internet-of-things," *IEEE Internet Things J.*, 10.1109/JIOT.2019.2954678, 2019.
- [12] H. Guo, Q. Zhang, S. Xiao, and Y.-C. Liang, "Exploiting multiple antennas for cognitive ambient backscatter communication," *IEEE Internet Things J.*, vol. 6, no. 1, pp. 765–775, 2019.
- [13] Q. Zhang, H. Guo, Y.-C. Liang, and X. Yuan, "Constellation learning-based signal detection for ambient backscatter communication systems," *IEEE J. Sel. Areas Commun.*, vol. 37, no. 2, pp. 452–463, 2019.
- [14] Q. Zhang, L. Zhang, Y. Liang, and P. Kam, "Backscatter-NOMA: A symbiotic system of cellular and Internet-of-Things networks," *IEEE Access*, vol. 7, pp. 20000–20013, 2019.
- [15] R. Long, H. Guo, L. Zhang, and Y. Liang, "Full-duplex backscatter communications in symbiotic radio systems," *IEEE Access*, vol. 7, pp. 21 597–21 608, 2019.
- [16] H. Guo, Y.-C. Liang, R. Long, S. Xiao, and Q. Zhang, "Resource allocation for symbiotic radio system with fading channels," *IEEE Access*, vol. 7, pp. 34 333–34 347, 2019.
- [17] Q. Zhang, Y.-C. Liang, and H. V. Poor, "Intelligent user association for symbiotic radio networks using deep reinforcement learning," *arXiv preprint arXiv:1905.04041*, 2019.
- [18] Y.-C. Liang, R. Long, Q. Zhang, J. Chen, H. V. Cheng, and H. Guo, "Large intelligent surface/antennas (LISA): Making reflective radios smart," *J. Commun. Inf. Netw.*, vol. 4, no. 2, pp. 40–50, 2019, also available at arXiv:1906.06578.
- [19] S. Gong, X. Lu, D. T. Hoang, D. Niyato, L. Shu, D. I. Kim, and Y.-C. Liang, "Towards smart radio environment for wireless communications via intelligent reflecting surfaces: A comprehensive survey," *arXiv preprint arXiv:1912.07794*, 2019.
- [20] S. Liu, T. J. Cui, A. Noor, Z. Tao, H. C. Zhang, G. D. Bai, Y. Yang, and X. Y. Zhou, "Negative reflection and negative surface wave conversion from obliquely incident electromagnetic waves," *Light: Sci. & Appl.*, vol. 7, no. 5, p. 18008, 2018.

- [21] Q. Wu and R. Zhang, "Intelligent reflecting surface enhanced wireless network: Joint active and passive beamforming design," in *2018 IEEE Global Communications Conference (GLOBECOM)*. IEEE, Dec. 2018, pp. 1–6.
- [22] —, "Intelligent reflecting surface enhanced wireless network via joint active and passive beamforming," *IEEE Trans. Wireless Commun.*, 2019.
- [23] C. Huang, A. Zappone, G. C. Alexandropoulos, M. Debbah, and C. Yuen, "Reconfigurable intelligent surfaces for energy efficiency in wireless communication," *IEEE Trans. Wireless Commun.*, vol. 18, no. 8, pp. 4157–4170, 2019.
- [24] J. Chen, Y. Liang, Y. Pei, and H. Guo, "Intelligent reflecting surface: A programmable wireless environment for physical layer security," *IEEE Access*, vol. 7, pp. 82 599–82 612, 2019.
- [25] G. Yang, X. Xu, and Y.-C. Liang, "Intelligent reflecting surface assisted non-orthogonal multiple access," *arXiv preprint arXiv:1907.03133*, 2019.
- [26] Z. Ding and H. V. Poor, "A simple design of IRS-NOMA transmission," *arXiv preprint arXiv:1907.09918*, 2019.
- [27] S. Zhang and R. Zhang, "Capacity characterization for intelligent reflecting surface aided MIMO communication," *arXiv preprint arXiv:1910.01573*, 2019.
- [28] C. Pan, H. Ren, K. Wang, W. Xu, M. ElKashlan, A. Nallanathan, and L. Hanzo, "Multicell MIMO communications relying on intelligent reflecting surface," *arXiv preprint arXiv: 1907.10864*, 2019.
- [29] Q. Wu and R. Zhang, "Weighted sum power maximization for intelligent reflecting surface aided swipt," *IEEE Wireless Commun. Lett.*, DOI: 10.1109/LWC.2019.2961656, 2019.
- [30] Z.-Q. He and X. Yuan, "Cascaded channel estimation for large intelligent metasurface assisted massive mimo," *IEEE Wireless Commun. Lett.*, DOI: 10.1109/LWC.2019.2948632, 2019.
- [31] A. Taha, M. Alrabeiah, and A. Alkhateeb, "Enabling large intelligent surfaces with compressive sensing and deep learning," *arXiv preprint arXiv:1904.10136*, 2019.
- [32] L. Boccia, F. Venneri, G. Amendola, and G. Di Massa, "Application of varactor diodes for reflectarray phase control," in *IEEE Antennas Propag. Soc. International Symposium*, vol. 3. IEEE; 1999, 2002, pp. 132–135.
- [33] D. Tse and P. Viswanath, *Fundamentals of wireless communication*. Cambridge university press, 2005.
- [34] J.-F. Bousquet, S. Magierowski, and G. G. Messier, "A 4-GHz active scatterer in 130-nm CMOS for phase sweep amplify-and-forward," *IEEE Trans. Circuits Syst. I, Reg. Papers*, vol. 59, no. 3, pp. 529–540, 2011.
- [35] B. R. Marks and G. P. Wright, "A general inner approximation algorithm for nonconvex mathematical programs," *Oper. Res.*, vol. 26, no. 4, pp. 681–683, Jul./Aug. 1978.
- [36] Q. Li, M. Hong, H.-T. Wai, Y.-F. Liu, W.-K. Ma, and Z.-Q. Luo, "Transmit solutions for MIMO wiretap channels using alternating optimization," *IEEE J. Sel. Areas Commun.*, vol. 31, no. 9, pp. 1714–1727, 2013.
- [37] M. Grant, S. Boyd, and Y. Ye, "CVX Users Guide," *Tech. Rep.*, 2009.
- [38] S. Boyd and L. Vandenberghe, *Convex optimization*. Cambridge university press, 2004.
- [39] Y. Nesterov and A. Nemirovskii, *Interior-point polynomial algorithms in convex programming*. Siam, 1994, vol. 13.
- [40] A. A. Nasir, H. D. Tuan, T. Q. Duong, and H. V. Poor, "Secrecy rate beamforming for multicell networks with information and energy harvesting," *IEEE Trans. Signal Process.*, vol. 65, no. 3, pp. 677–689, 2016.
- [41] Z. Luo, W. Ma, A. M. So, Y. Ye, and S. Zhang, "Semidefinite relaxation of quadratic optimization problems," *IEEE Signal Process. Mag.*, vol. 27, no. 3, pp. 20–34, May 2010.
- [42] R. A. Horn and C. R. Johnson, *Matrix analysis*. Cambridge university press, 2012.